CHALMERS
UNIVERSITY OF TECHNOLOGY

Maraging steel fatigue properties processed by forging and additive manufacturing.

A comparative study on Uddeholms AB Corrax® and Corrax AM® steels

Master's thesis in Materials Engineering

TOMÁS M. THORBURN CARRETERO

Department of Industrial and Materials Science
CHALMERS UNIVERSITY OF TECHNOLOGY
Gothenburg, Sweden 2019

Master's thesis 2019: 55119

Maraging steel fatigue properties processed by forging and additive manufacturing

A comparative study on Uddeholms AB Corrax® and Corrax AM® steels.

TOMÁS M. THORBURN CARRETERO

CHALMERS
UNIVERSITY OF TECHNOLOGY

Department of Industrial and Materials Science
Division of Engineering Materials
Chalmers University of Technology
Gothenburg, Sweden 2019

Maraging steel fatigue properties processed by forging and additive manufacturing
A comparative study on Uddeholms AB Corrax® and Corrax AM® steels.
TOMÁS M. THORBURN CARRETERO

© TOMÁS M. THORBURN CARRETERO, 2019.

Supervisor: Johan Ahlström, Department of Industrial and Materials Science
Industry Supervisor: Christos Oikonomou, Uddeholms AB
Examiner: Johan Ahlström, Department of Industrial and Materials Science

Master's Thesis 2019: 55119
Department of Industrial and materials science
Division of Engineering Materials
Chalmers University of Technology
SE-412 96 Gothenburg
Telephone +46 31 772 1000

Typeset in LaTeX
Gothenburg, Sweden 2019

Fatigue properties assessment for different manufacturing methods on Maraging steel
Uddeholms AB Corrax® and Corrax AM® fatigue properties are quantified and comparatively assessed
TOMÁS M. THORBURN CARRETERO
Department of Industrial and Materials Science
Chalmers University of Technology

Abstract

Fatigue properties for three different manufacturing processes of the same material are studied. The material is Corrax® and Corrax AM®, a maraging steel from Uddeholms AB. The three different batches representing the three different manufacturing methods include the reference Corrax® batch and two Powder bed laser fused Corrax AM® batches one of which is hipped and the other is not. All the batches are heat treated to achieve maximum hardness levels. Further tests are performed on the batches to understand the behavior of the material and the influence of the manufacturing processes on the material's properties.
The results show no statistical meaningful difference between the batches in terms of low cycle fatigue performance. However microstructure, defects present and mechanical properties show differences.

Keywords: Fatigue, Additive Manufacturing, Powder bed laser melting, Hot isostatic pressing, Maraging steel.

Acknowledgements

I would like to thank everybody involved in the making of this thesis.
Johan and Christos thank you for your good supervision and guidance through the whole process. Elanghovan thank you for your help with everything related to the tensile machine and your help with matlab. Thanks to Chalmers University for providing me with everything necessary. To all the guys in Uddeholm thank you for making me feel like at home during the time I stayed in Hagfors.
As this thesis represents the end of my masters degree and my time at Chalmers I would like to thank everybody who made it possible for me to come to Sweden and study. My supportive family; my mother and father, Iain and Carol, Javi and Nacho. Family friends like Mark and Carl. Thank you for your support.
Thanks to all my friends for making everything fun. And thanks specially to you, Maria.

Tomás M. Thorburn, Gothenburg, September 2019

Contents

List of Figures

List of Tables

1
Introduction

1.1 Background

Uddeholms AB, a global company with headquarters in Hagfors, Sweden is the world's leading manufacturer of tool steel for industrial molds and other applications. One of their strategic interests is know-how and product development [1]. Uddeholms AB operates in a competitive market where higher quality is expected from manufacturing processes and from such demand the need for understanding of their steels and products is derived.
Additive Manufacturing (AM) is defined by the American Society for Testing Materials (ASTM) as the "process of joining materials to make objects from three dimensional (3D) model data, usually layer upon layer as opposed to subtractive manufacturing technologies"[2]. This project focuses in the Powder Bed Laser Melting (PBLM) process from all those included in AM. PBLM uses a laser as energy source to selectively melt a pattern on a bed of metal powder forming a layer, this layer is melted on the previous layer and the next layer will be melted over it, gradually forming the 3D object. [3]
Another technology that often plays a role combined with PBLM and other AM methods is High Isostatic Pressure (HIP). HIP in the context of AM technologies aims to minimize some of the PBLM defects such as porosity or partially unmelted zones. In our case, the PBLM manufactured object is placed inside a pressurized chamber where temperature is increased. The aim is to create a driving force for these defects to re-melt and be eliminated or at least reduced. [5]
PBLM offers many advantages in many fields such as the aeronautical or medical field, for a tool steel manufacturer such as Uddeholms AB one of their main interests lays on the manufacturing of alloys for plastic extrusion and injection molds. The quality of the plastic component being manufactured by these molds depends, amongst other things, in the temperature control of the mold. This is achieved by cooling channels within the mold. For complex geometries these channels are often only possible by PBLM. Uddeholms AB currently offers an alloy in powder form to meet such market demand, Corrax AM®. This alloy was developed from the forged version, Corrax®. [1] [4]

1.2 Objective

This project aims to further extend the knowledge available on Corrax AM®. More specifically fatigue properties for this alloy in both hipped and not hipped conditions

and to reference them to the properties for Corrax®.

2
Theory

2.1 Material

This thesis focusses on the fatigue properties of a maraging steel manufactured by Uddeholms AB, its commercial name being Corrax® and Corrax AM®.

2.1.1 Chemical composition

The chemical composition of Corrax® and Corrax AM® is the same and is given in this table:

Table 2.1: Corrax® and Corrax AM® Chemical composition

Element	C	Si	Mn	Cr	Ni	Mo	Al	Fe
weight%	0.03	0.3	0.3	12.0	9.2	1.4	1.6	Balance

2.1.2 Microstructure and heat treatments

In contrast to the brittle martensite obtained upon quenching in high carbon tool steels, maraging steels produce very soft martensite upon quenching from the austenitic phase present above 850ºC. The Fe–Ni alloy produces body centered cubic (BCC) martensite which is very ductile. This soft martensite is then strengthened by ageing of the martensite at elevated temperatures.
Elements such as Titanium or Aluminium form different kinds of thermally stable intermetalics that precipitate in the martenisitic structure during this ageing. These intermetallics noticeably strengthen the martensitic phase. The combination of martensite and aging give the name of maraging steels.[11]
Carbon is kept low so it does not form Titanium Carbides which severely reduce the impact strength, ductility and toughness when present in high concentration. [11]
Chromium provides the stainless grade to the steel by means of forming a cohesive chromium oxide passive layer, this is crucial for the steel application.
The general heat treatment which allows a maraging steel to have a great combination of strength and ductility is divided in two parts.
First a homogenization, solution or austenization heat treatment is given, for Corrax® and Corrax AM® Solution HT should be done at 850ºC with a holding time of 30 minutes and cooling in air [6][7]. The obtained microstructure is Martensitic, some amount of retained austenite can also be present. This material's state is referred to as the soft state or delivery condition, machining take place in this state.

Its hardness is 34 HRC in delivery state.[6][7]
After Solution HT, the next heat treatment is given. This is called Ageing or Precipitation hardening heat treatment (PH HT). For Corrax® and Corrax AM® final hardness and properties can be trimmed by means of modifying the ageing HT temperature and holding times. Cooling is done in air.

Table 2.2: Different Ageing HT options [6][7]

Ageing temperature/time	*Hardness (HRC)*
No apply solution HT	34
525°/4h	49 - 52
575°/4h	44 - 47
600°/4h	40 - 42

For this project all batches are aged to give maximum hardness levels (49-52 HRC)

2.1.3 Properties

Some of the most relevant mechanical properties as specified in references [6] and [7] are:

Table 2.3: Corrax® and Corrax AM® mechanical properties at room temperature [6][7]

State	Solution treated (34 HRC)	Aged (40 HRC)	Aged (46 HRC)	Aged (50 HRC)
$Rp_{0.2}(MPa)$	700	1000	1400	1600
$UTS(MPa)$	1100	1200	1500	1700

Additionally powder properties such as Sphericity, Aspect Ratio and densities for Corrax AM® can be found in reference [7].

2.1.4 Applications

The combination of the mechanical properties shown before and excellent corrosion resistance make Corrax® and Corrax AM® suitable for moulds which will work with corrosive plastics, rubber or food; extrusion dies; Plastic processing or Engineering components [6][7].

2.1.5 Material batches

To fulfill the project´s objective three different material batches are manufactured and tested. These batches represent the different optimum material service conditions.

Batch 1, also referred to as reference batch. This Batch corresponds to Corrax®. The samples belonging to this batch belong to the normal production Corrax® Uddeholms AB produces at their Hagfors mill. It has therefore been manufactured following the same high standards and has a fully traceable history. The material is forged with cylindrical shape from where samples are obtained aligned with the forging direction. Both homogenization heat treatment and ageing heat treatment (ageing HT) were performed by Uddeholms AB to obtain the testing condition for the batch at maximum hardness level.
Batches 2 and 3 are both Corrax AM®. The samples start their life as Corrax AM® powder which is then PBLF printed in an EOS M270 machine. Print parameters are those which have been proven optimal for this alloy, the aim of this thesis is not to study print parameters influence on fatigue so these parameters are not discussed. All the samples were printed in two different build jobs and then mixed for experiment randomization purposes. Up to this stage there is no manufacturing difference between batch 2 and 3, they both belong to the same powder batch and their printing parameters are the same. Powder data and printing parameters are fully traceable.
Batch 2 is subjected to a solution HT and an ageing HT aiming to obtain maximum hardness levels.
Batch 3 follows a Hipping stage after printing; during the hipping the material is also homogenized. Finally, the batch undergoes the same ageing HT as Batch 2. A total amount of 30 samples are manufactured for this project, 10 for each batch.
Samples belonging to Batch 1 are noted with the letter R followed by a number from 1 to 10. The 10 samples are equivalent and no positional difference exists, this is ensured by Uddeholms AB quality control.
Samples belonging to Batches 2 and 3 are denoted with two numbers X-Y.The first number X defines the sample´s position within the build plate (X goes from 1 to 10). The second number Y defines the build job (Y is either 1 or 2). This nomenclature is needed as inconsistency within PBLF exists. There can be inconsistencies from one build to an other. There can also be inconsistencies for different positions of the samples on the build plate within the same build plate. For instance samples that are further away from the recoater or the Argon input could receive a different powder and argon supply. [8].
One of the differences between batches 2 and 3 is the cooling rate each batch is subjected after their solution HT or Hipping.
The following images shows the three different batches, their manufacturing processes, their nomenclature and how the samples are mixed for randomization purposes.

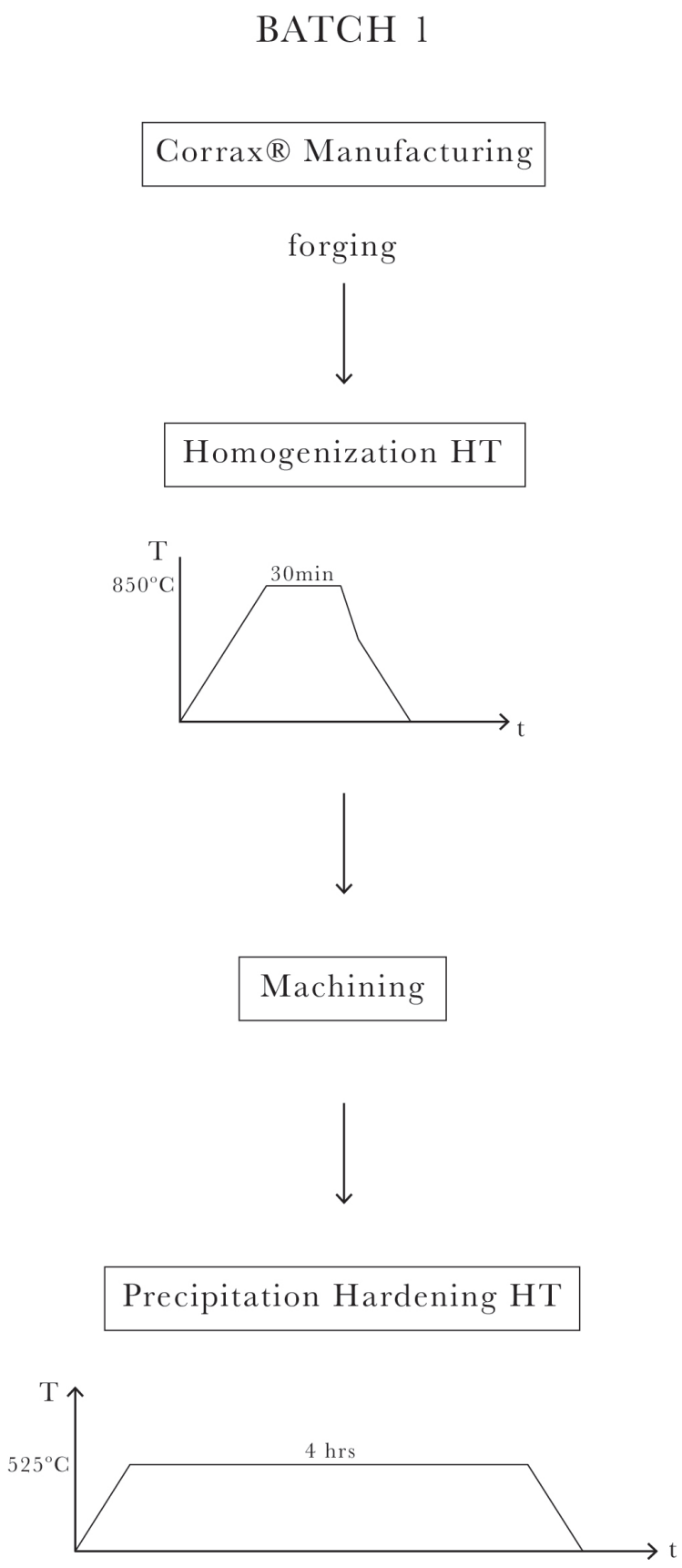

Figure 2.1: Batch 1 manufacturing process

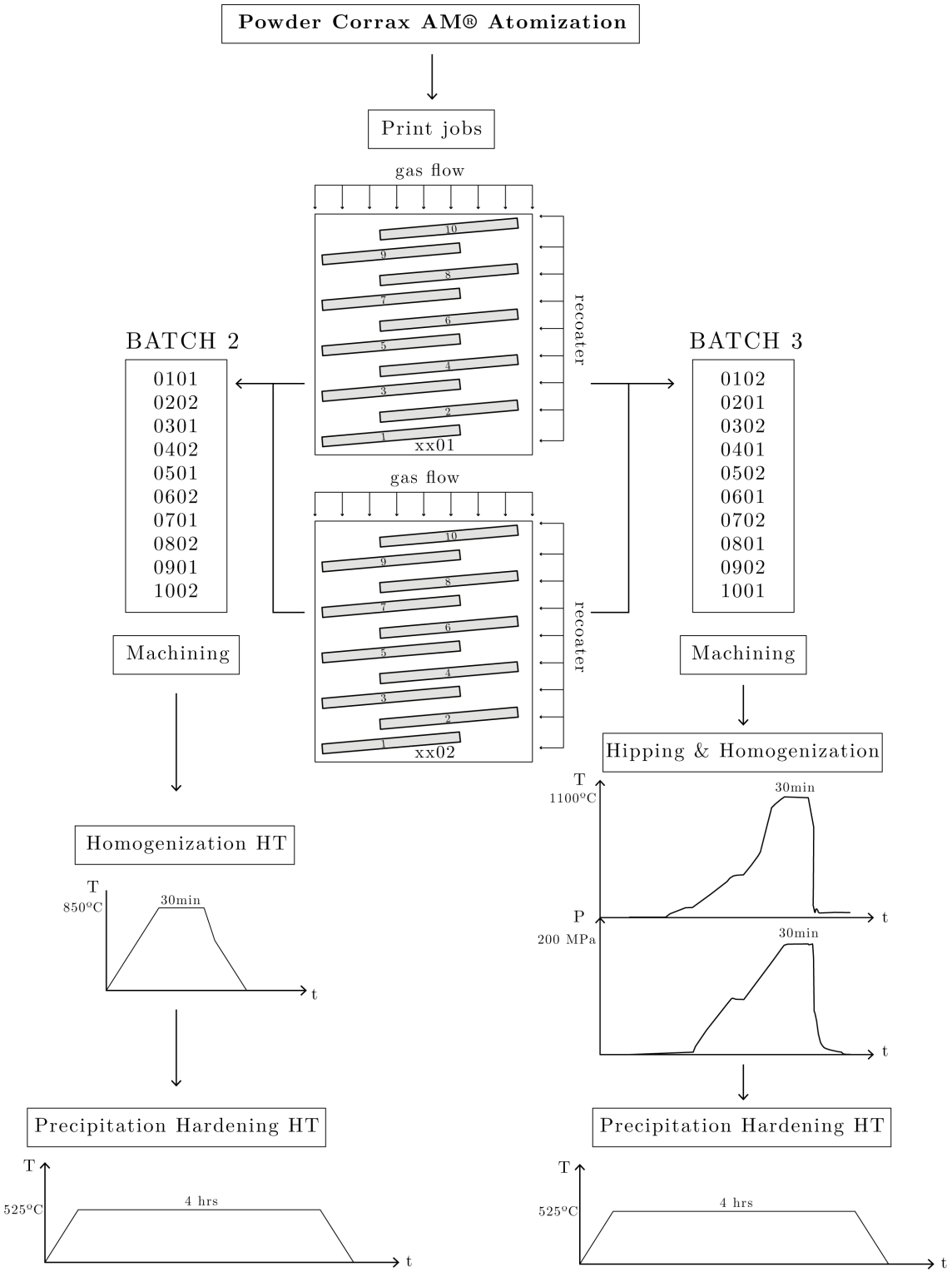

Figure 2.2: Batch 2 and 3 manufacturing process

2.2 Tensile Tests

A tensile test is the uniaxial tensile loading of a material sample. The testing conditions are forced so that the strain (ε) is increased continuously causing an elastic, then plastic deformation and finally rupture.
The load on the sample and the strain at each moment is measured and recorded. Load is measured with a load cell and so is strain with an extensometer. Load is converted into engineering stress (σ) using the sample's original diameter. Stress and strain provide valuable information about the different material batches:
Yield Stress. It is the stress above which permanent deformation is created in the material, up to this level of stress the material responds elastically, fully recovering its original shape when unloaded. Up to this stress level the material also follows a linear relationship between stress and strain, this relationship is known as Hooke's law. It is generally measured in MPa.
Young's Modulus or *E-Modulus* (E). It is the proportionality coefficient for Hooke's law. Graphically speaking it can be interpreted as the slope in the linear part of the Stress-Strain curve. It is normally measured in GPa.

$$\sigma = E\varepsilon$$

Tensile strength (UTS). It is the maximum stress the sample can sustain. Up to this point and after yield stress the sample has deformed plastically but homogeneously, after UTS is reached a neck is formed and the deformation is no longer homogeneous on all of the sample's length. It is generally measured in MPa.
The strain at which yield stress occurs will be denoted as strain at yield (ε_y). Similarly, the strain at which UTS happens can be defined as strain at UTS (ε_{UTS}).
The region between Yield stress and UTS is of particular interest for the following fatigue tests.
Other parameters not so interesting for this study can be obtained from the Stress-Strain curve such as *fracture strain*, percentage of elongation and energy absorbed or area under the curve.

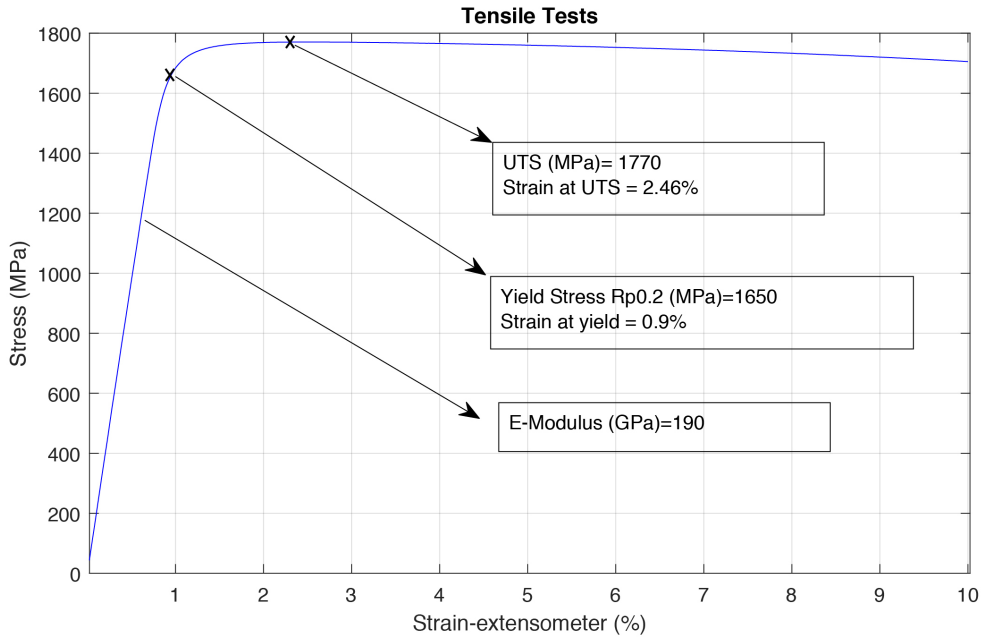

Figure 2.3: Stress-Strain curve for sample R1 belonging to Reference Batch

2.3 Fatigue Tests

Fatigue in metallic materials can be described as the behavior of the material to a repetitive or cyclic stress. The initial stress is not enough to cause failure but cyclically loading this stress ultimately causes failure, there is therefore damage accumulation from the cyclic loading. This damage is normally manifested as a crack that forms and grows.
Fatigue is usually divided in three stages. Crack initiation, stable crack growth, and unstable crack growth which causes failure. Crack initiation is particularly susceptible to surface defects or stress concentrators as these normally originate in the surface. This is the reason samples are polished until a mirror-like surface is obtained as recommended by [2].
To determine a material's response to fatigue, samples are loaded cyclically under controlled stress or strain. Ours will be strain controlled and the stresses will be an output signal. To cyclically load the material means it will be forced from its initial state of zero stress and strain to a certain strain ε_{max} where it will be experiencing a certain stress (σ_{max}), then unloading of the sample and further loading (if necessary) to reach ε_{min} and σ_{min}, finally the first cycle is completed by loading again the sample. Normally ε_{max} and ε_{min} are chosen so that plastic deformation happens, the hysteresis loop is therefore widened by the time it is closed. The following image illustrates this first loop and the stress and strain definitions including amplitudes ε_a σ_a and plastic strain amplitude $\Delta\varepsilon_p$:

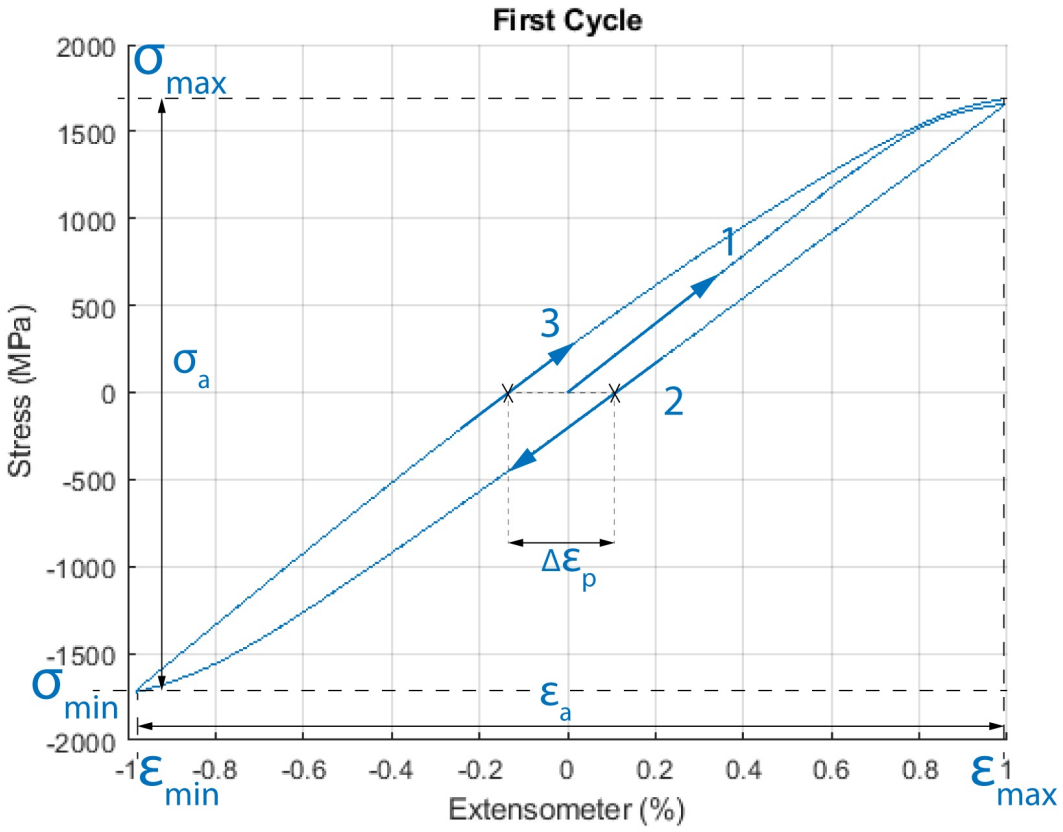

Figure 2.4: First loading cycle for sample R8 showing the different stress and strains defined previously.

Fatigue tests are normally referred to as high or low cycle fatigue tests. The main difference is the amount of cycles the samples run at, higher that 10^5 is normally considered high cycle fatigue (HCF). HCF tests run for many cycles because they are normally run only within the material´s elastic range. Low cycle fatigue (LCF) are such that a certain amount of plastic deformation is obtained with each cycle, thus ε_{max} is higher than ε_{yield} or in terms of stress, σ_{max} is often higher than σ_{yield} / $Rp_{0.2}$. Our tests will be LCF and strain controlled as previously mentioned.
Similarly to tensile tests, stress and strain are measured and recorded continually with a load cell and extensometer. Along with other data obtained the so called Coffin-Mason equation for a material can be elaborated. This equation gives the relation between number of cycles to failure $2N$ and plastic strain amplitude $(\Delta\varepsilon_p)/2$. The Coffin-Manson equation can thus be useful to anticipate life cycles for a given plastic strain or the other way round.[12]

$$(\Delta\varepsilon_p)/2 = \varepsilon'_f(2N)^c$$

Where the *ductility coefficient* ε'_f and the *fatigue ductility exponent* c are constants.

3
Experimental

3.1 Tensile Tests

3.1.1 Test objective

Tensile tests are performed to obtain useful information about the material that will be then used for the following fatigue testing. The desired information is Strain at Yield ε_p and Strain at Necking ε_{UTS} as well as other data such as Elastic modulus E and Stresses: Plastic Yield Stress σ_{yield}, Ultimate tensile strength UTS.

3.1.2 Specimens and sample preparation

The specimens used for the tensile tests are no different from those subjected to the following LCF tests.
The dimensions, as recommended in ASTM E606 [2], to which samples are machined from the respective material batches are shown in the following image. The position of the samples from the bulk material is parallel to the forging direction for batch 1.

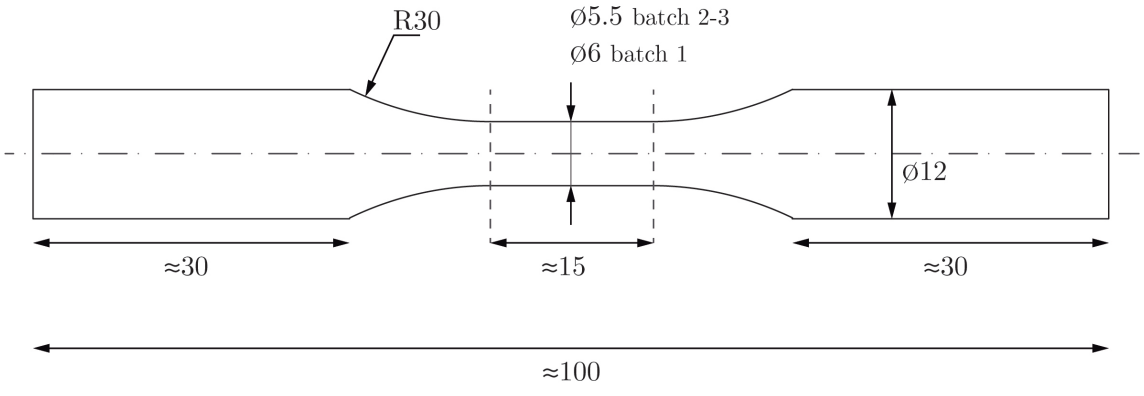

Figure 3.1: Sample dimensions in mm for batches 1, 2 and 3

Samples are received after being machined and then aged, superficial corrosion and machining marks are therefore present on the samples. To obtain a mirror like finish as recommended in ASTM E606 [2] samples are ground and then polished with a structured method. The result is a polished surface with marks and scratches as

shown in Table 4.13.

3.1.3 Test Conditions

One specimen per material batch is tested.
The tests are all performed at room temperature, controlled by the laboratory´s facilities. Humidity is disregarded as this stainless steel shows no effect to ambient moisture. [6][7].
The tests are performed on an Instron 8501 machine, using a 50kN maximum force cell, a 10% maximum elongation extensometer and mechanical grips suitable for the specimen´s diameter. The software used was to control the machine and measure the outputs is provided by MTS.
The strain rate is the same as the one that will be used for fatigue testing, $2\times10^{-4}s^{-1}$.

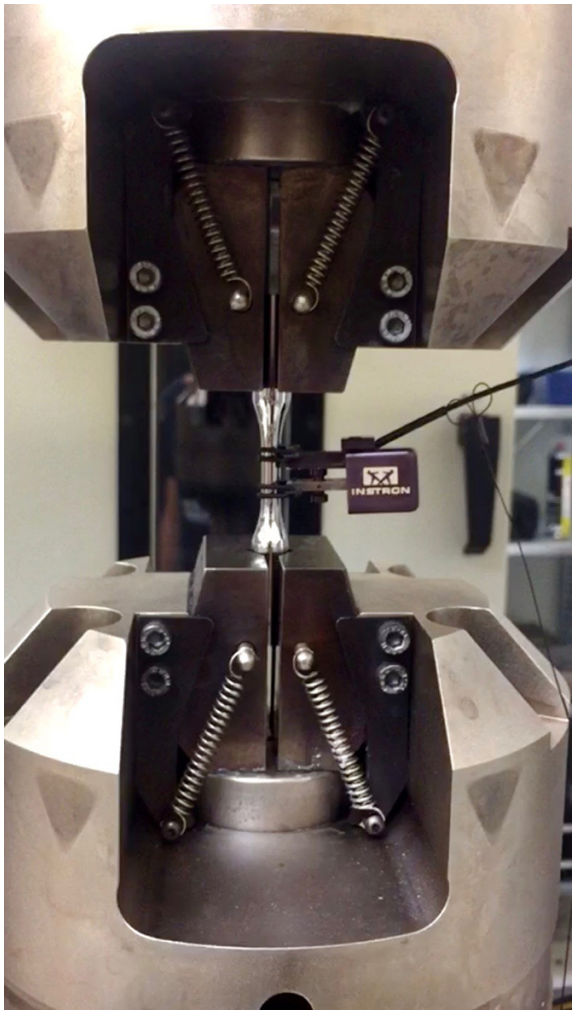

Figure 3.2: Sample held by the Instron mechanical grips and extensometer installed

3.2 Fatigue Tests

3.2.1 Objective

The fatigue tests aim to distinguish whether performance differences on cyclic loading exist between the three material batches. The tests also aim to produce experimental data to quantify and describe the materials´ behavior to cyclic loading.

3.2.2 Specimens

As mentioned in previously fatigue samples are no different geometrically speaking from those used in tensile testing and present the same surface finish.
The samples dimensions and surface finish follow ASTM E606 [2] recommendations.

3.2.3 Testing conditions

All the tests are strain controlled. This means the sample will travel between certain levels of strain, strain amplitude, imposed by the machine and the force will be registered as an output.
After performing the tensile test (see Tensile Tests Results) on the different batches, three different strain amplitude levels are chosen; these are 0.6%, 0.8% and 1.0% for all of the three batches.
Temperature, humidity and the hardware and software used for fatigue testing is the same as for the tensile tests. Only the appropriate program being run is changed from test to test depending on the strain amplitude being tested. The strain rate for the first cycle on each test is $5 \times 10^{-3} s^{-1}$ then, for the following cycles, the strain rate is the same as the one that was used for tensile testing, $2 \times 10^{-2} s^{-1}$. This means the following triangular shape input signal for the strain controlled tests:

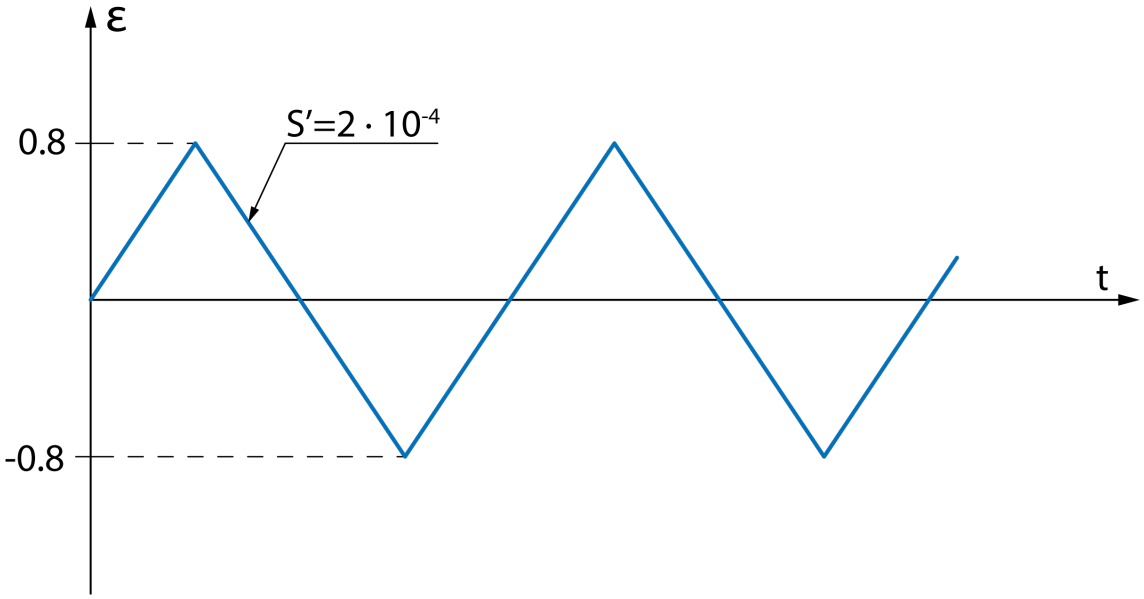

Figure 3.3: Input signal for a 0.8% strain amplitude controlled LCF test. Strain rate is $2 \times 10^{-2} s^{-1}$

For randomization purposes the samples are also mixed when being tested, as can be seen in the results chapter.

3.3 Hardness testing

3.3.1 Objective

The aim of hardness testing is to gather information about the different batches´ properties. Hardness measuring can also be used to evaluate the batches´ different heat treatments.

3.3.2 Testing conditions

Hardness testing is performed on a Struers automatic macro hardness machine. Five measurements are taken per sample for statistical consistency. Temperature and humidity remain lab controlled.

3.3.3 Samples

The samples used for hardness testing belong to the three batches. Some of the intermediate stages of the batches´ manufacturing processes of Corrax AM® are also hardness tested, this is done to further understand the differences throughout the manufacturing processes. Samples are flat and polished to at least 1600 grit paper.

3.4 X-Ray Difractometry

3.4.1 Objective

X-Ray Difractometry (XRD) is used here to evaluate the amount of retained austenite present in the material. Austenite is a soft phase in this material, hinders mechanical performance and is obtained by a not fast enough cooling rate of the material from its Solution HT. Therefore determining the amount of retained austenite in the material allows us to know if the cooling rate was fast enough and make the evaluation of different fabrication processes possible.

3.4.2 Working principle

A sample is subjected to an incident X-Ray beam. A certain amount of the beam is partially diffracted and measured, this will be the intensity. As the X-ray emitting device and receiver are rotated over a 2 spectrum a randomized measurement is obtained over the whole measuring area. Different crystallographic cells diffract differently. This means the body centered cubic martensite can be distinguished from the face centered cubic austenite. The austenite fraction is measured as a ratio between the austenite and martensite peak intensities.

Figure 3.4: XRD machine and its main parts

3.4.3 Testing conditions

The tests were performed at Uddeholms AB by a qualified operator.

Table 3.1: XRD testing conditions details

Anodmaterial	Cr
Voltage	40kV
Current	35mA
Wavelength A1	2.2897500Å
Wavelenght A2	2.2936600Å
Detector	Position sensitive detector (PSD)
Filter	V
Scan	2θ - area (50^o - 168^o), step length (0.1^o), measuring time (60s), speed=0.1^o/s, $2nm$ collimator,Ω varying 25.1^o to 80.725^o.
PSD Accumulation	12
Oscillation (χ)	Oscillate, Amplitude 90^o, Speed = 4^o/s
Rotation (Φ)	Continuous, Speed 14^o/s

3.4.4 Sample

Samples include not only the final fatigue testing stages but also the intermediate steps along the fabrication of the sample to better understand when the austenite is formed and its evolution.
Sample preparation included electropolishing in order to avoid mechanical deformation on the surface affecting the results.

3.5 Micrography

3.5.1 Objective

Micrography samples are prepared to qualitatively asses microstructure differences between batches due to their different manufacturing processes.

3.5.2 Sample preparation

Samples are selected from all three batches and some of their intermediate stages of manufacturing to gather information about the material´s microstructure evolution. These samples are mounted on bakelite and polished to mirror finish. Then following [13] they are etched in Villella and also in sodium picrate.

3.5.3 Testing conditions

Although not strictly a test, samples are mounted and photographed on a calibrated microscope, different magnifications are used. Grain size is also checked using a grid

available on the microscope.

3.6 Fractography

3.6.1 Objective

The aim by assessing the fracture surfaces on the fatigue samples is to gather information regarding the material batches´ rupture mechanisms. The objective is to clarify the crack initiation point/s, the crack growth area, the type of rupture and if the crack propagates through the grains and/or their boundaries.

3.6.2 Experimental

Under fractography analysis three different evaluating methods are included, their main difference being the magnification achieved: visual evaluation, Stereomicroscope and SEM. See Chapter XX on equipment used.

3.6.3 Samples

All samples subjected to fatigue testing and which fracture surfaces remain unaltered are studied as fractography samples by visual inspection and stereomicroscope. Afterwards some samples are introduced in the SEM for further analysis at higher magnification.

3.7 Defect evaluation

3.7.1 Objective

The aim is to evaluate the density, size, shape and size distribution of defects present in the different material batches. Defects such as inclusions play an important role in fatigue properties; such defects can lead to crack initiation points and help propagate cracks [9].

3.7.2 Experimental

In order to fulfill the objective a defect count is performed on the different material batches. The experimental procedure is that specified by the Swedish standard SS 111116 [10] and is carried out by a qualified operator at Uddeholms AB.
SEM is also used to provide images of the defects found and EDX to analyze their composition.

3.7.3 Samples

Samples for defect count are flat samples embedded in bakelite and polished to mirror finish using the Struers automatic polishing machine, this same samples can then be introduced for SEM and EDX analysis.
Three samples from each of the AM batches are subjected to defect count. Only one sample from the reference batch is subjected to defect count as numerous references on the defects present in this production run material exist. Along with the final batches, samples from intermediate stages of manufacturing are also analyzed, as it also done with Hardness and XRD measurements. This is done to further understand the defects evolution through the manufacturing process of Batches 2 and 3.
The total surface area examined and magnification used is specified in the results chapter as well as the exact sample the measurements come from.

3.8 Surface roughness

3.8.1 Objective

Verify that the sample preparation done on all fatigue samples leave a similar surface finish, ensuring this way little to none influence of surface roughness on the fatigue performance.

3.8.2 Samples

One sample from each batch is selected. R6 from batch 1, 0101 from batch 2 and 0301 from batch 3.

3.8.3 Testing conditions

The specimens were analyzed with a BRUKER ContourGT optical microscope system in combination with the Vision64® metrology application.
Only 1 field of view (FOV) is used to eliminate stitching errors and complex shape variations as values are in the nm range. A 40x magnification was used with vertical resolution below 0.1nm. Surface is flattened in the software to take out form errors. All values are measured by Bruker´s Stylus analysis application. Cutoff is 0.25 mm (5 cutoff lengths used). The results are an average of two measurements taken.

4

Results

4.1 Tensile tests

Table 4.1: $Rp_{0.2}$, σ_{UTS} and ε_{UTS} results from Tensile Tests

	Batch 1 Sample R1	Batch 2 Sample 0202	Batch 3 Sample 0501
$Yield\,Stress\,(MPa)$	1650	1600	1475
$UTS\,(MPa)$	1770	1720	1615
ε_{UTS}	2.46	1.70	4.12

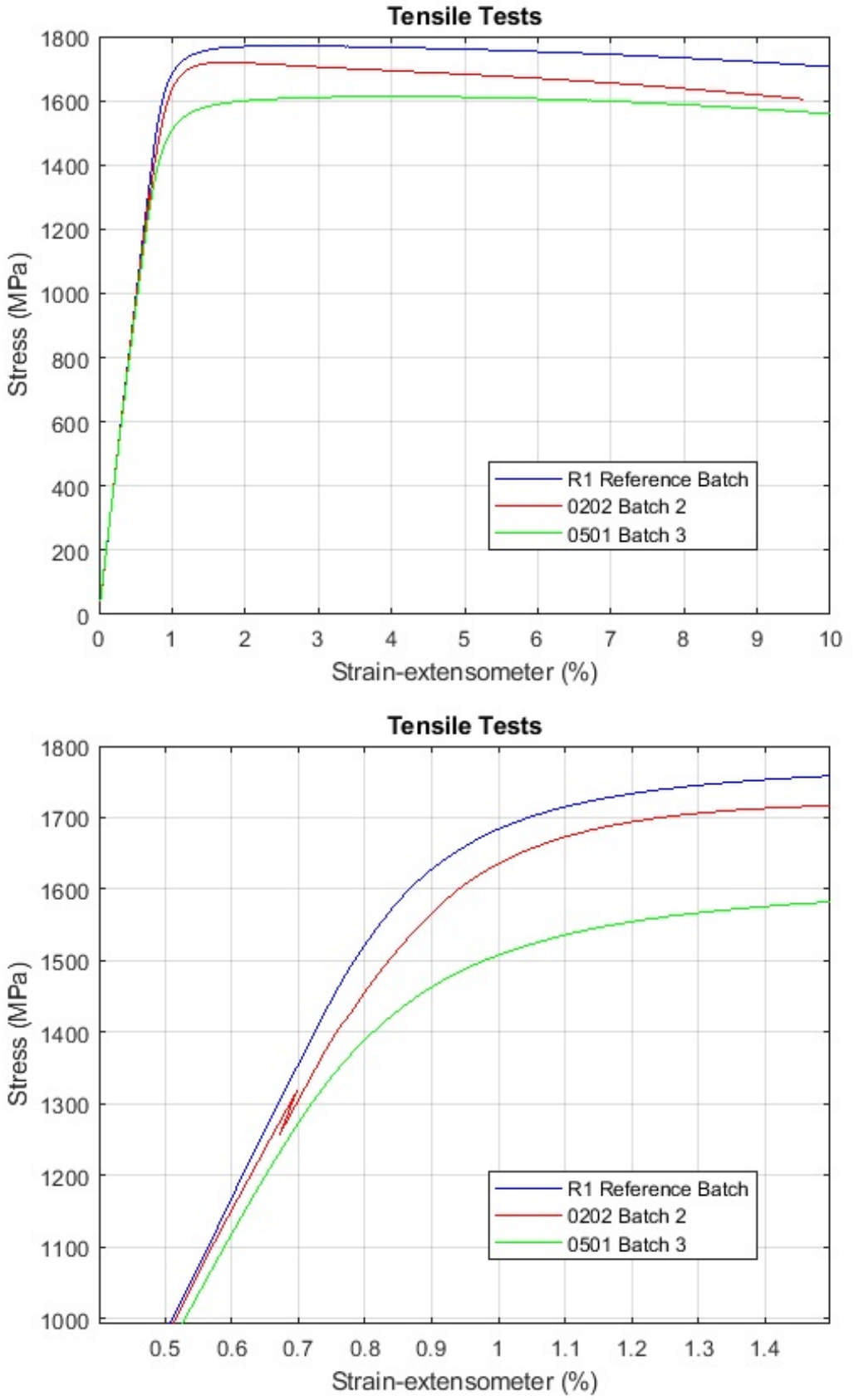

Figure 4.1: Stress-Strain curves for batches 1,2 and 3 and detail

4.2 Fatigue Tests

4.2.1 Summary tables

Table 4.2: LCF summary table for batch 1 samples

Sample Name	*Amplitude* $\Delta\varepsilon/2$	*Cycles*
$R1$	Tensile test	
$R2$	1.0%	137
$R8$	1.0%	483
$R9$	1.0%	401
$R4$	0.8%	1887
$R6$	0.8%	724
$R3$	0.6%	13892
$R5$	0.6%	7411
$R7$	Not valid	
$R10$	Not valid	

Table 4.3: LCF summary table for batch 2 samples

Sample Name	*Amplitude* $\Delta\varepsilon/2$	*Cycles*
0401	Tensile test before correct HT	
0202	Tensile test	
0302	1.0%	252
0601	1.0%	180
0802	Not valid	
0101	0.8%	1187
1002	0.8%	547
0701	0.8%	1850
0502	0.6%	20010
0901	0.6%	13852

Table 4.4: LCF summary table for batch 3 samples

Sample Name	*Amplitude* $\Delta\varepsilon/2$	*Cycles*
0501	Tensile test	
0301	1.0%	173
0602	1.0%	126
0801	1.0%	300
0102	0.8%	600
1001	0.8%	1283
0201	0.8%	884
0402	0.6%	5611
0902	0.6%	9144
0702	Buckling at 1.2% not valid	

4.2.2 Hysteresis loops

For every sample that has been tested for fatigue the following hysteresis loops have been drawn: first loop, first five loops, five half life loops and five last loops. All of these graphs are included in the Appendix section.
The graphs are generated by analyzing the data files with a Matlab code.

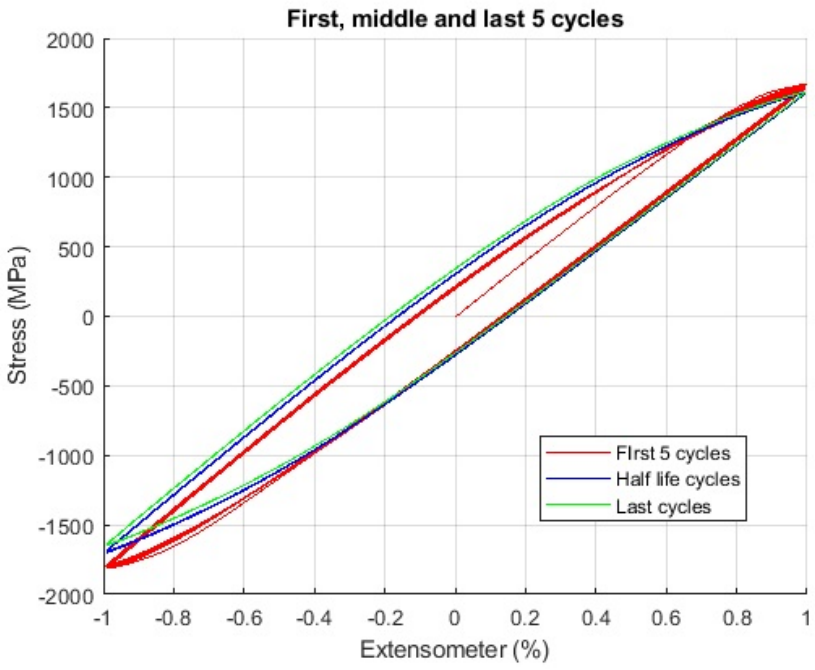

Figure 4.2: Sample 0601, Batch 2. Strain amplitude 1.0%

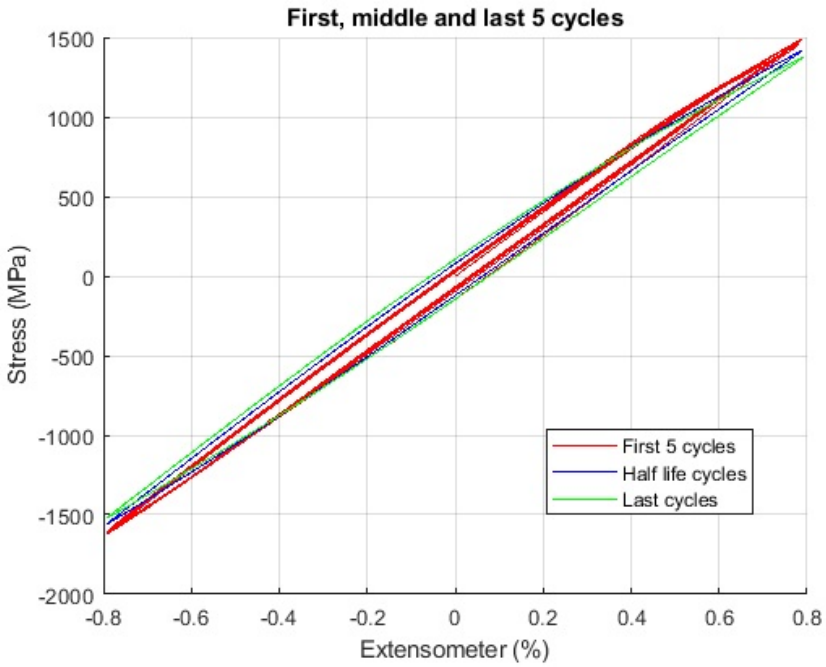

Figure 4.3: Sample 0701, Batch 2. Strain amplitude 0.8%

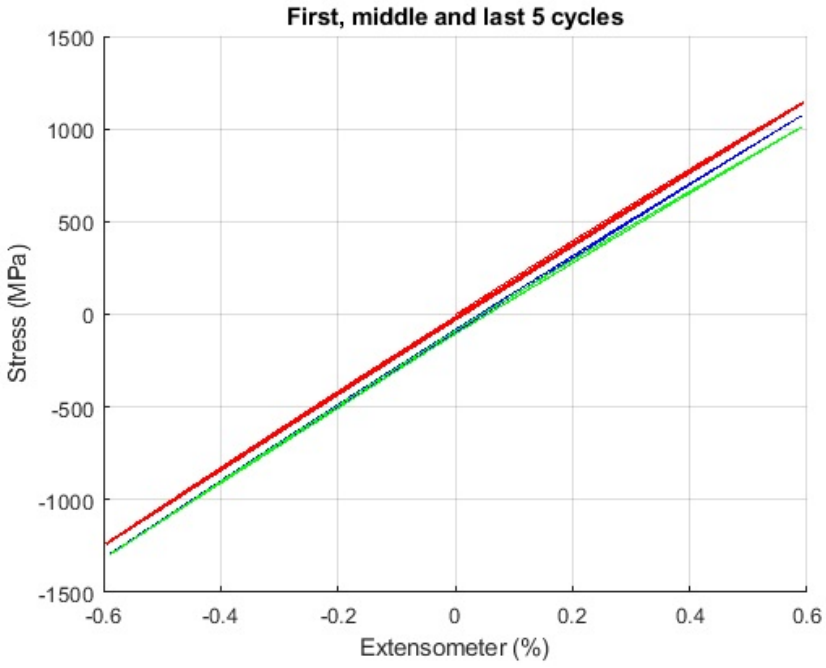

Figure 4.4: Sample 0502, Batch 2. Strain amplitude 0.6%

4.2.3 Stress Amplitude to Number of cycles

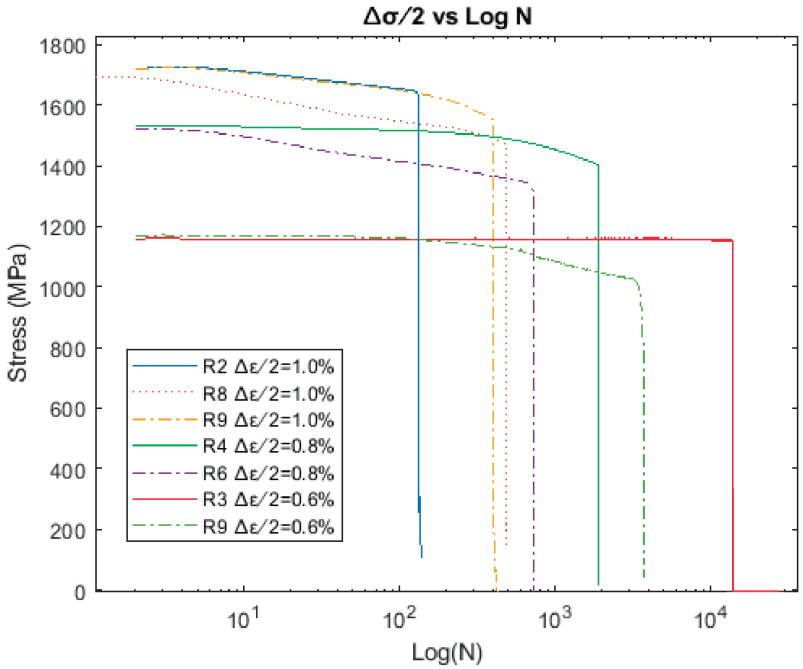

Figure 4.5: Stress Amplitude to number of cycles for Batch 1

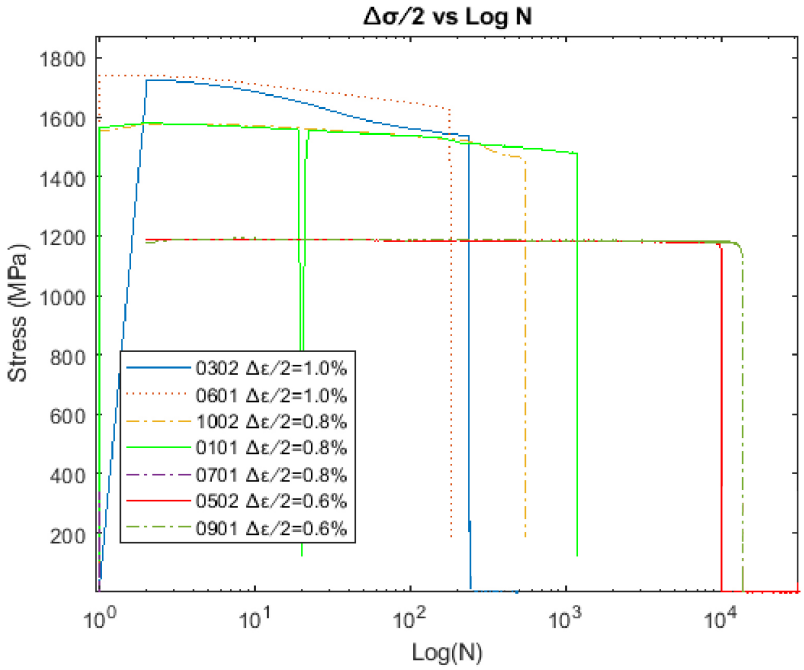

Figure 4.6: Stress Amplitude to number of cycles for Batch 2

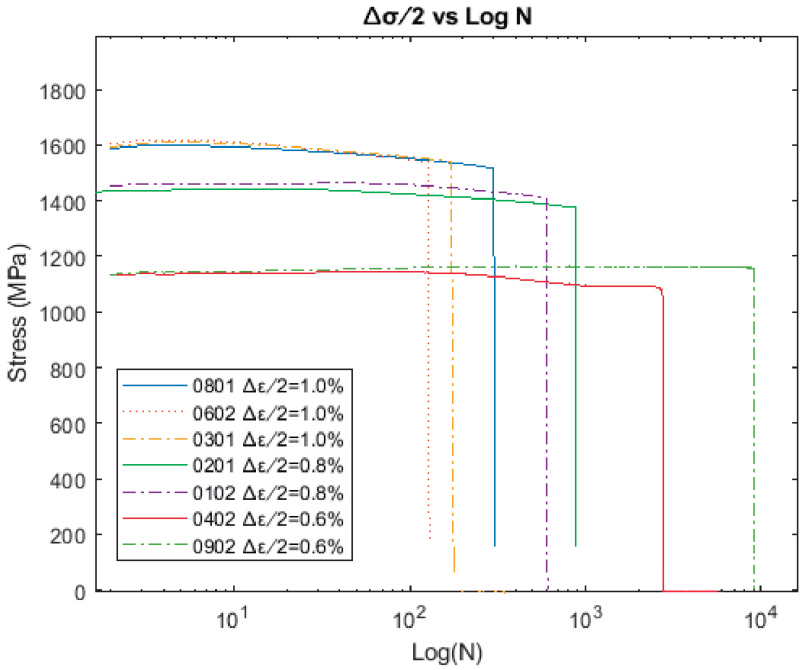

Figure 4.7: Stress Amplitude to number of cycles for Batch 3

4.2.4 Coffin-Manson equations

First the Coffin-Manson equations where all samples have been used to construct the fit are shown:

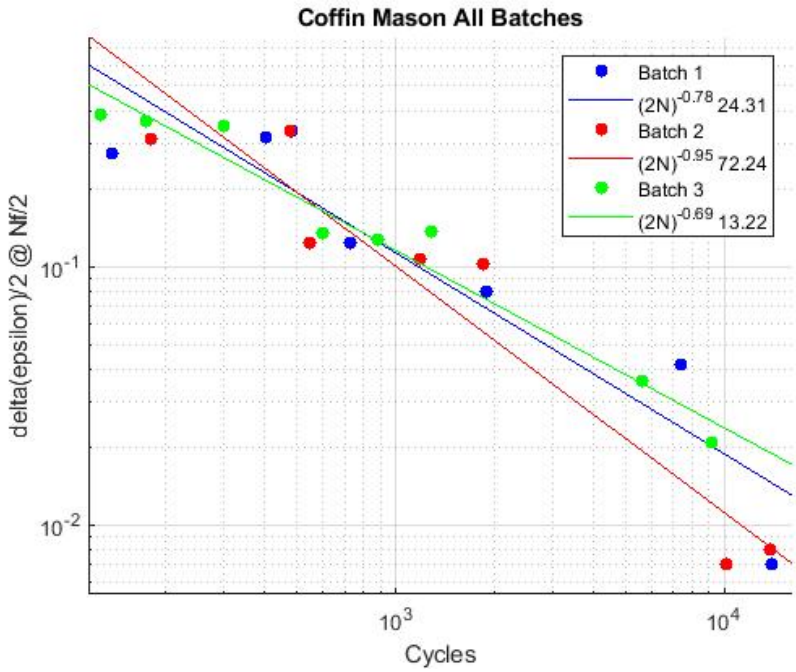

Figure 4.8: Coffin-Manson equations for all Batches using all samples available.

But the fit is poor due to 0.6% strain amplitude samples having too much scatter. In

the following C-M plot these samples are ignored. Additionally the 95% confidence interval for Batch 1 is also represented.

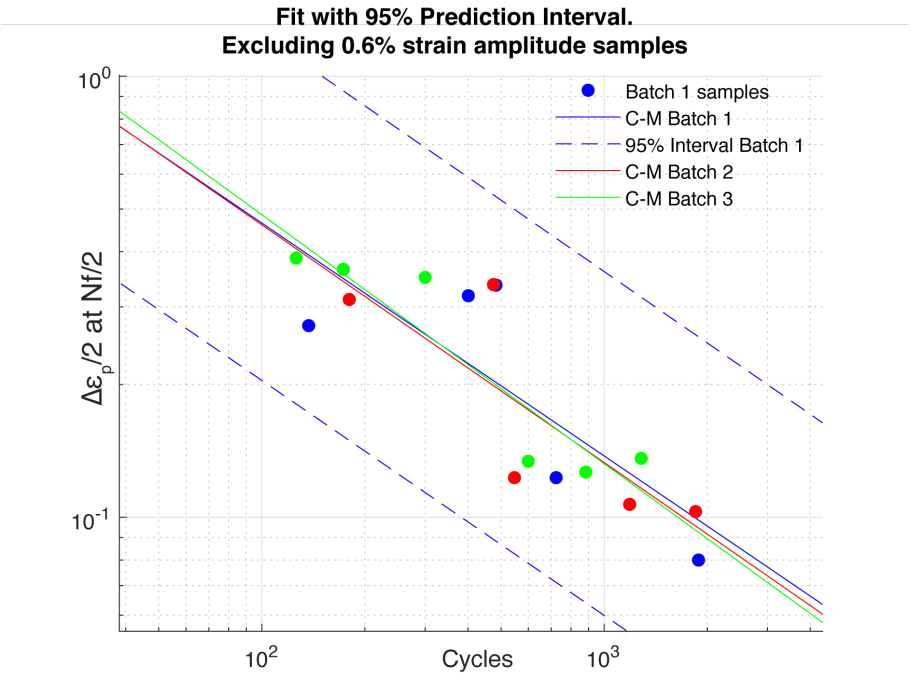

Figure 4.9: Coffin-Manson equations for all Batches using 0.8% and 1.0% strain amplitude samples.

The following table summarizes the C-M equations for all the batches excluding 0.6% samples.

Table 4.5: Coffin-Manson equation $\Delta\varepsilon/2 = (2N)^c \times \varepsilon'_f$ for all batches including only 0.8% and 1% strain amplitude samples

	ε'_f	c
Batch 1	5,28	-0,528
Batch 2	5,50	-0,539
Batch 3	6,53	-0,564

4.3 Hardness tests

Table 4.6: Macro-Hardness (HRC) for batches 1, 2 and 3. Five measurements are taken on each sample

	HRC	Standard deviation
Sample R7 Batch 1	51,8	0,173
Sample 0802 *Batch* 2	51,0	0,084
Sample 0702 *Batch* 3	49,64	0,173

Table 4.7: Macro-Hardness (HRC) measurements for intermediate stages of batches manufacturing

	HRC	Standard deviation
Sample 0901 *As Printed*	34,26	0,1704
Sample 0302 *As Printed*	34,88	0,0096
Sample 0401 *Printed + sol. HT*	34,70	0,1360
Sample 1002 *Printed + sol. HT*	34,86	0,0224
Sample 1001 *Hipped*	31,98	0,0216
Sample 0402 *Hipped*	32,34	0,0824

4.4 XRD Retained Austenite

Hardness values are also included for convenience.

Table 4.8: Retained Austenite for R7 (batch 1), 0802 (Batch 2) and 0702 (batch 3). HRC hardness values are also shown.

SAMPLE	*BATCH*	$A_R(\%)$	*HRC*
R7	1	1,8 (<2)	51,8
0802	2	$2{,}2 \pm 0{,}3$	51,0
0702	3	$4{,}5 \pm 0{,}5$	49,64

Table 4.9: Retained Austenite and HRC hardness values for different material´s manufacturing stages.

SAMPLE	*CONDITION*	$A_R(\%)$	*HRC*
0901	As printed	$22 \pm 1{,}3$	34,26
0302	As printed	$21 \pm 1{,}5$	34,88
0401	Printed + sol. HT	<2	34,70
1002	Printed + sol. HT	<2	34,86
1001	Hipped	$2{,}8 \pm 1{,}2$	31,98
0402	Hipped	$3{,}7 \pm 1{,}7$	32,34

4.5 Micrography

!

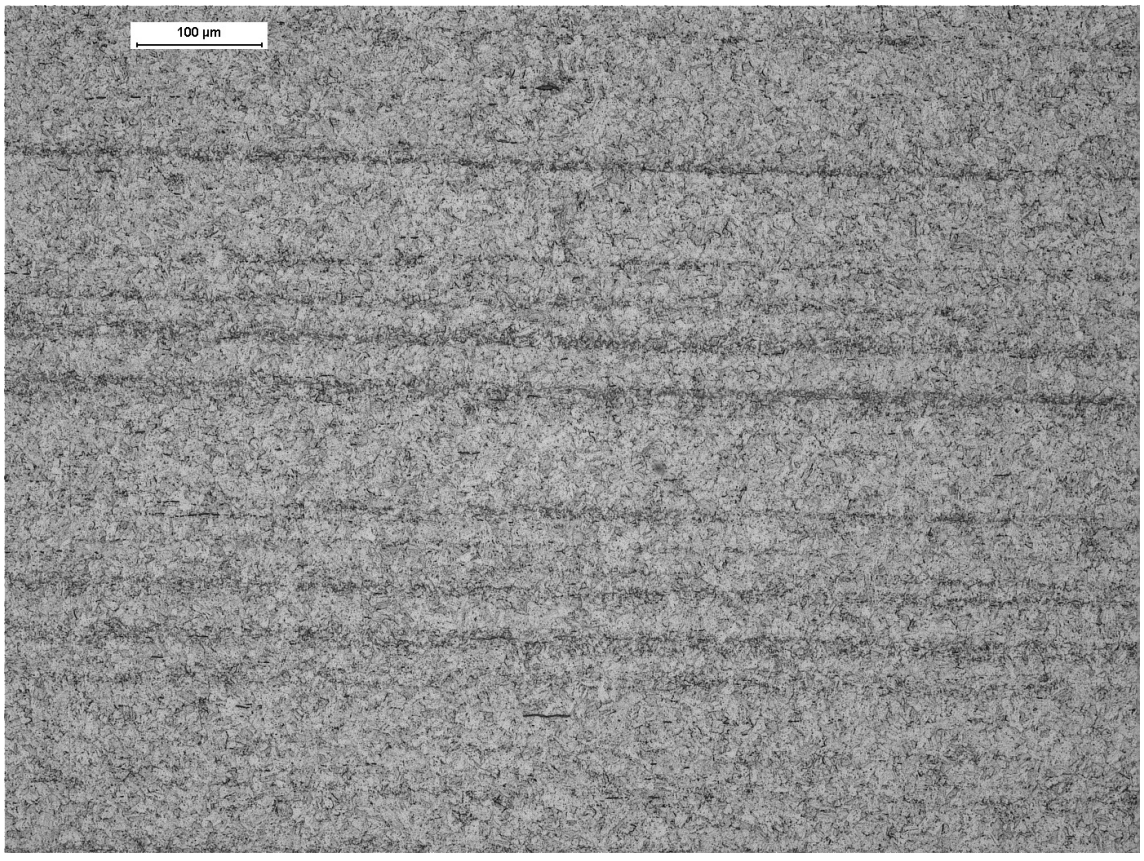

Figure 4.10: Batch 1 sample R7 Overall microstructure. Villella x100

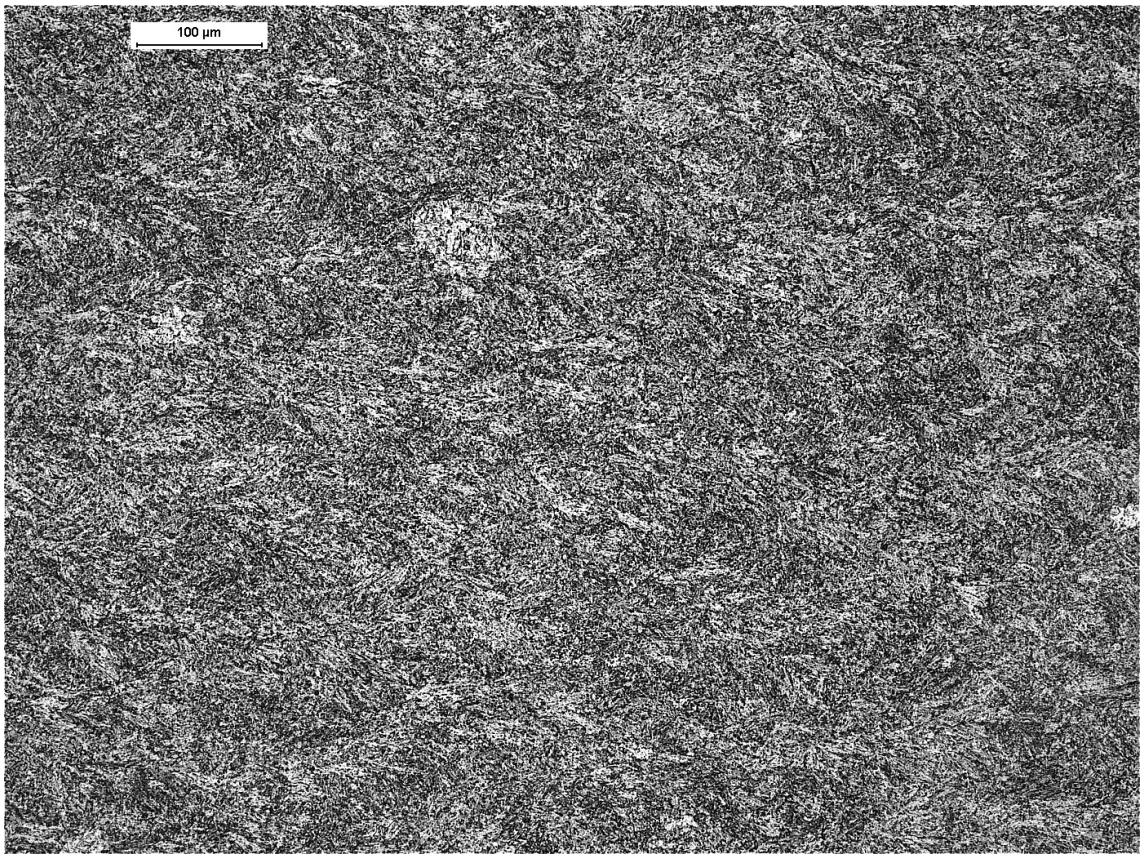

Figure 4.12: Batch 2 sample 0202. Overall microstructure. Villella x100

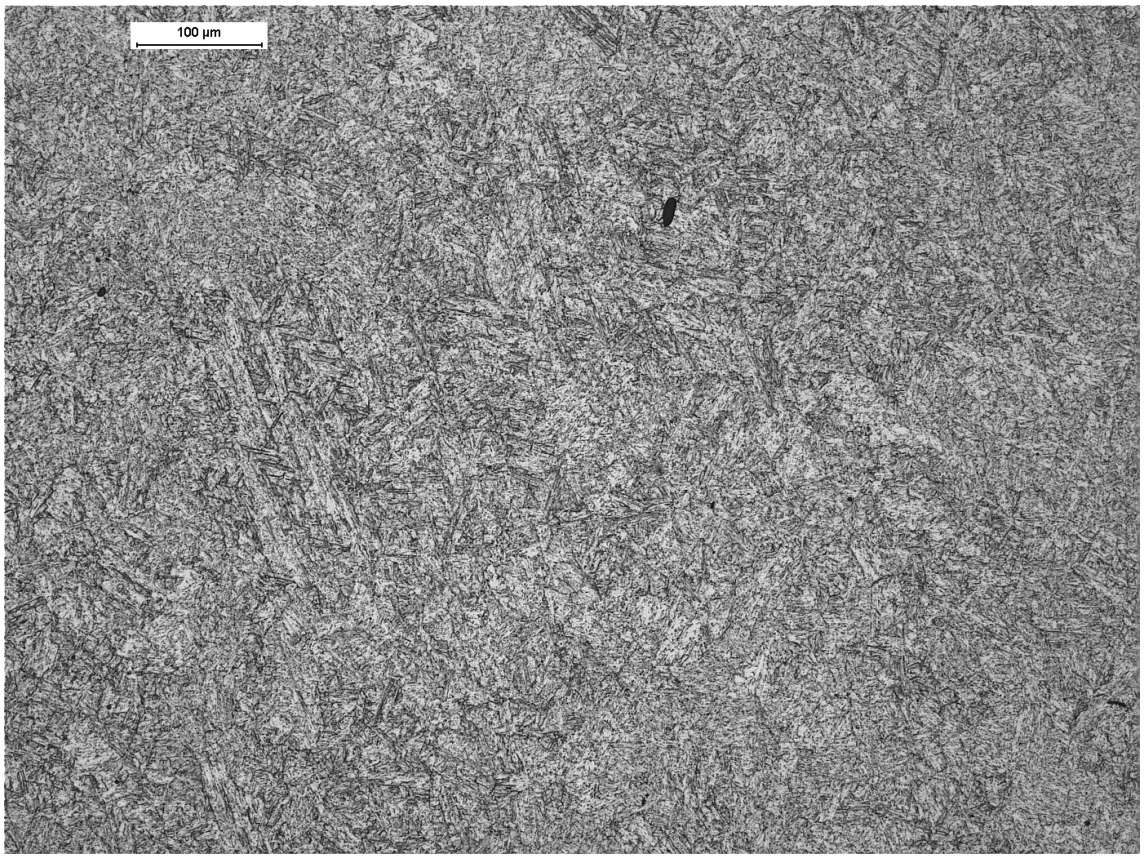

Figure 4.13: Batch 3 sample 0201 overall microstructure and defect. Villella x100

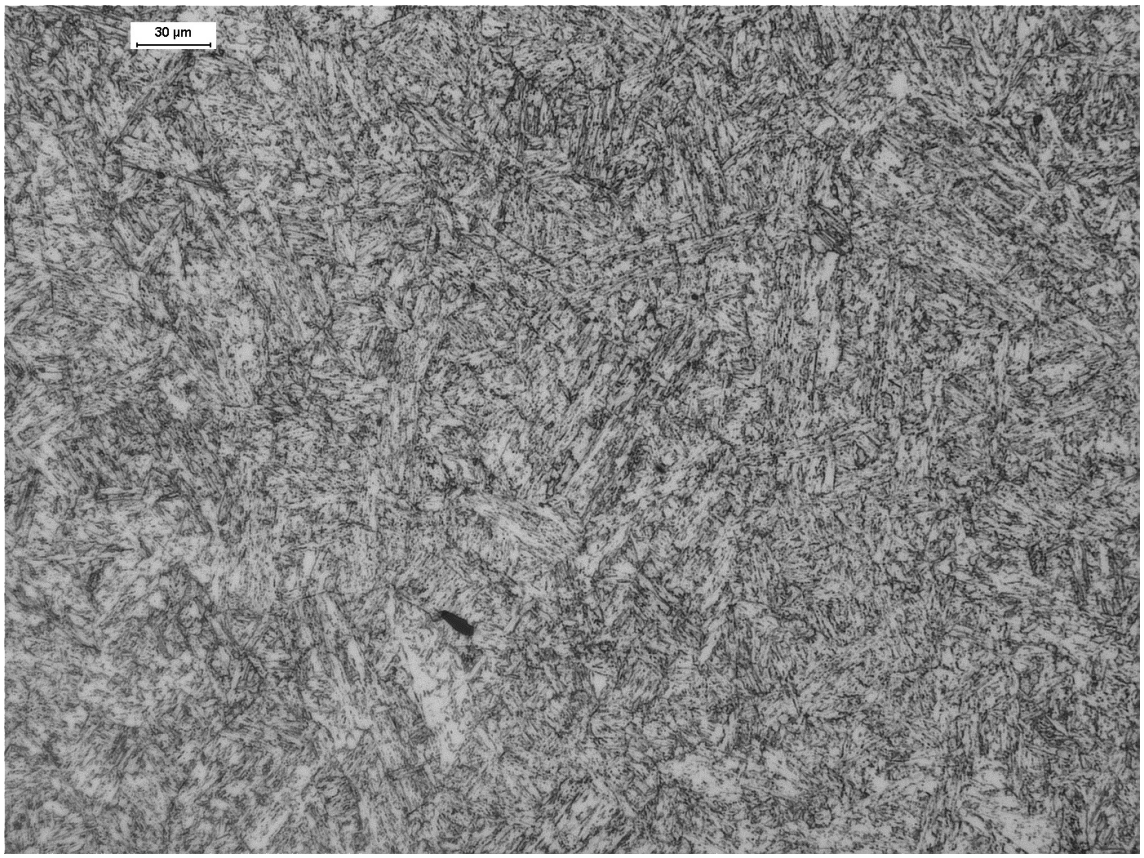

Figure 4.14: Batch 3 sample 0201 overall microstructure and defect. Villella x200

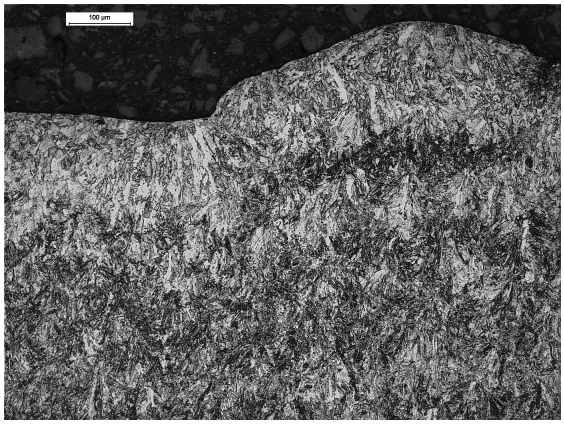

Figure 4.15: Sample 0901 Top layers as printed. Villella x100

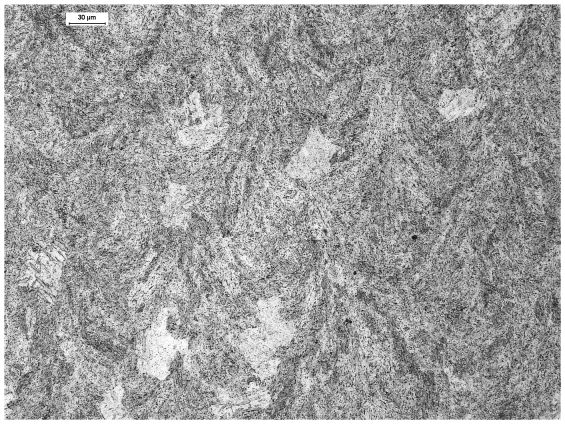

Figure 4.16: Sample 0401 Printed and Solution HT. Villella x100

4.6 Fractography

4.6.1 Stereo-microscope

All images of all the fracture surfaces are included in the Appendix section. As an example three samples from batch 3 showing larger crack propagation zone for

smaller strain amplitudes are shown.

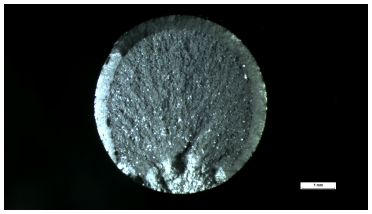

Figure 4.17: Sample 0902 Batch 3 tested at 0.6%

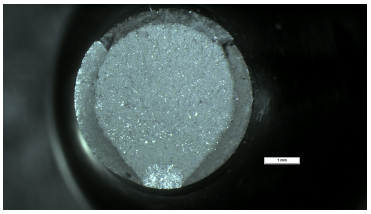

Figure 4.18: Sample 0102 Batch 3 tested at 0.8%

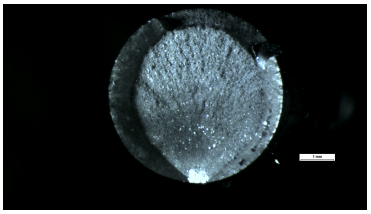

Figure 4.19: Sample 0301 Batch 3 tested at 1.0%

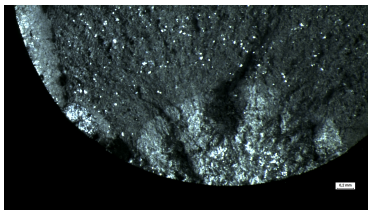

Figure 4.20: Close-up on sample 0902 Batch 3 tested at 0.6%

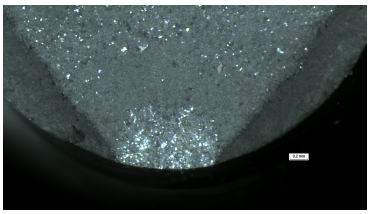

Figure 4.21: Close-up on sample 0102 Batch 3 tested at 0.8%

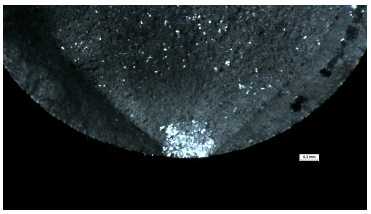

Figure 4.22: Close-up on sample 0301 Batch 3 tested at 1.0%

Fatigue samples can fracture because of the extensometer grip marks. The following images show this and the following table gathers this information.

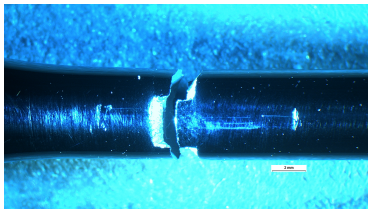

Figure 4.23: Fracture on sample 0201 happened between extensometer marks.

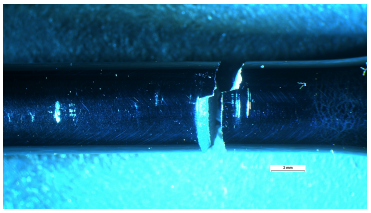

Figure 4.24: Fracture on sample 0101 happened on one of the extensometer marks.

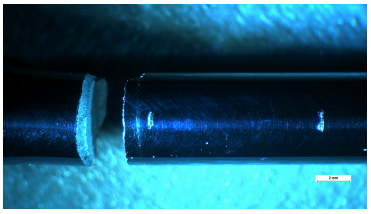

Figure 4.25: Fracture on sample 0902 happened out of the extensometer marks.

Table 4.10: Fractography breaking points

	Between ext. grip marks	On ext. grip marks	Out of ext. grip marks
R1	Tensile test		
R2	X		
R8	Non valid sample		
R9		X	
R4	X		
R6		X	
R3	X		
R5	X		
R7		X	
0401	Non valid sample		
0202	Tensile test		
0302	X		
0601		X	
0802			
0101		X	
1002			X
0701	X		
0502	X		
0901		X	
0501	Tensile test		
0301		X	
0602		X	
0801		X	
0102			X
1001		X	
0201	X		
0402	X		
0902		X	
0702	Missing buckling		

4.6.2 SEM images and EDX analysis

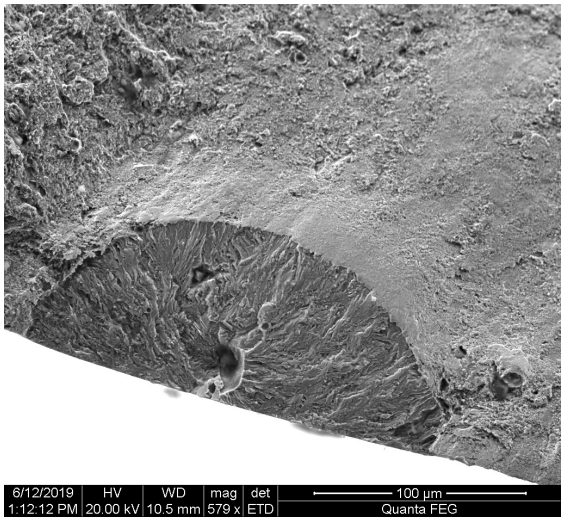

Figure 4.26: Crack growth area found on sample 0901.

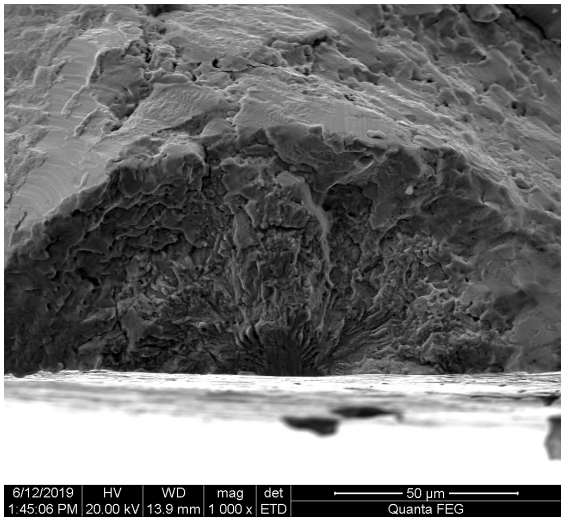

Figure 4.27: Crack initiation point found on sample R5.

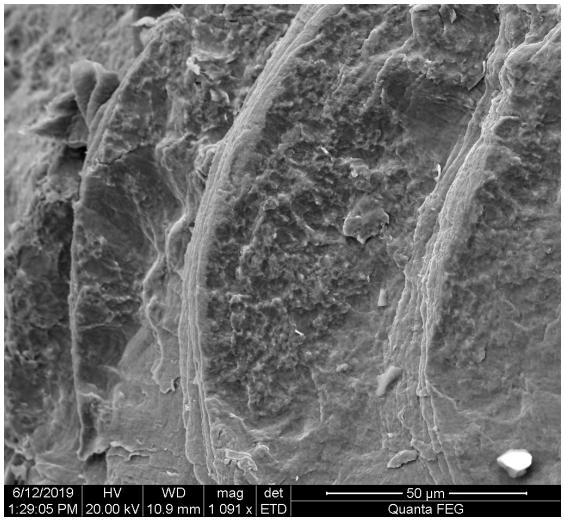

Figure 4.28: crack propagation features found on sample 0901.

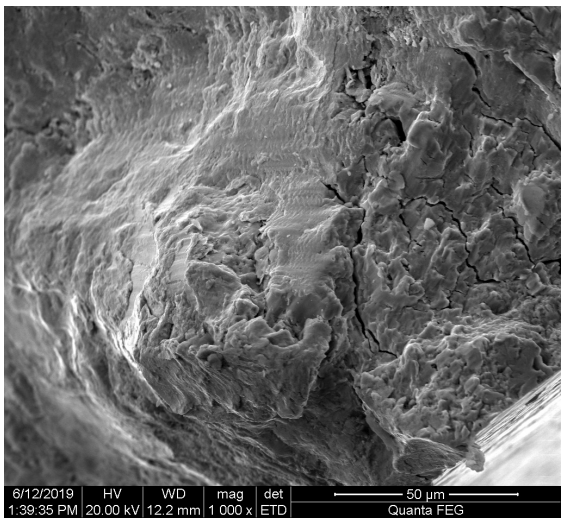

Figure 4.29: Crack propagation features and secondary fractures found on sample R5.

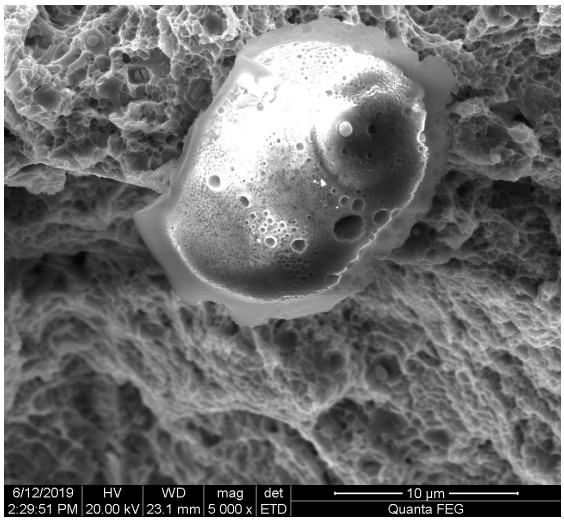

Figure 4.30: Alumina inclusion found on sample 0102.

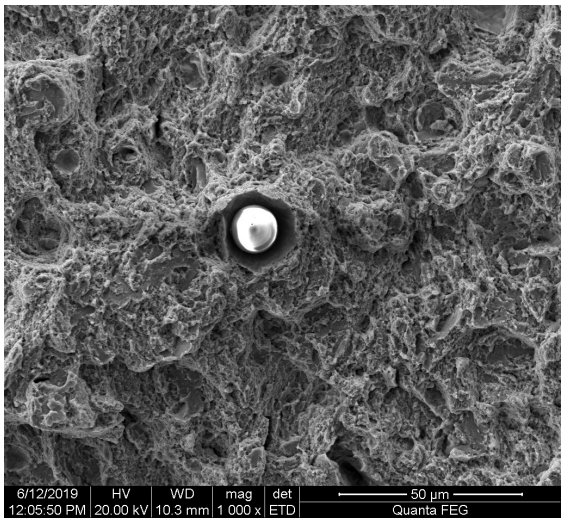

Figure 4.31: Spherical alumina inclusion found on sample 0101. Notice the softer matrix deformed surrounding it.

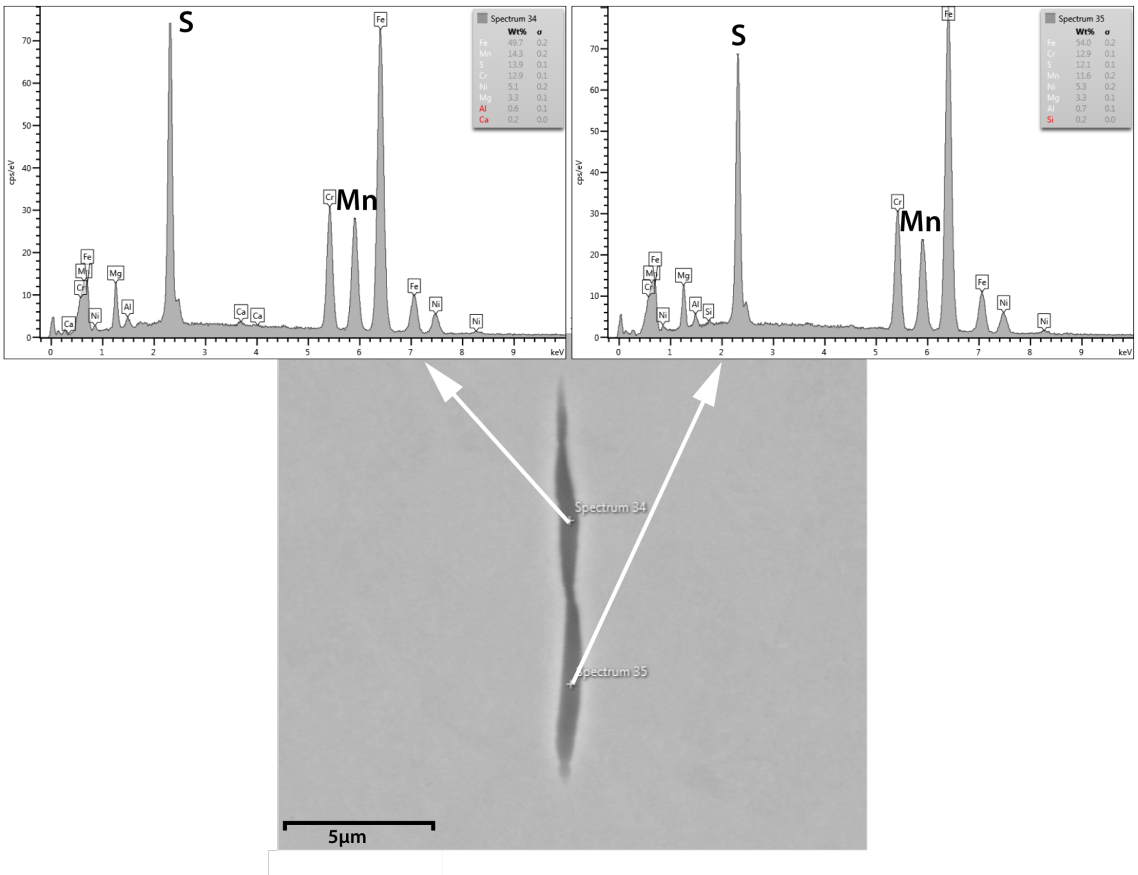

Figure 4.32: Defects in Batch 1. MnS stringer aligned with the forging direction

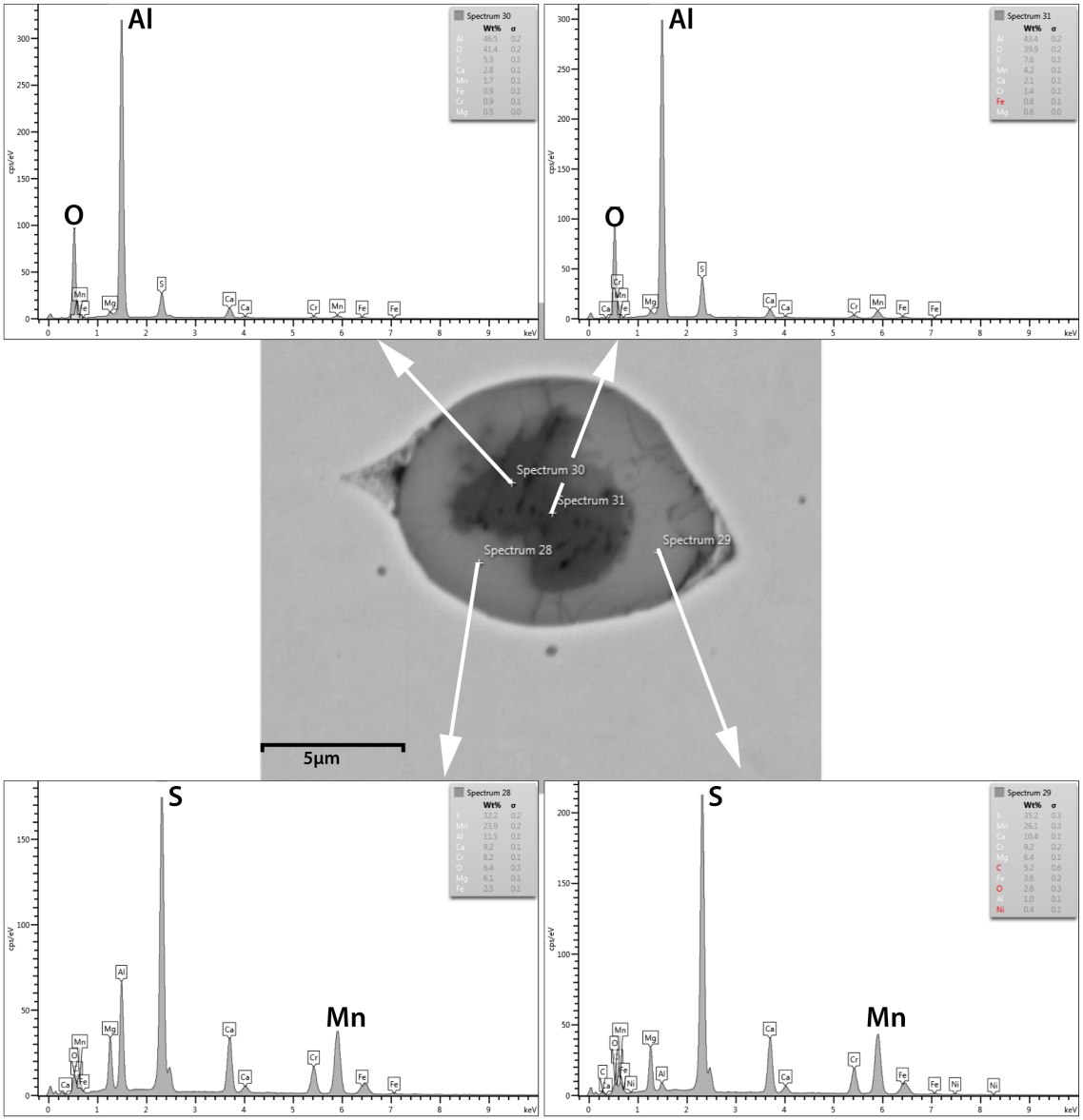

Figure 4.33: Defects in Batch 1. Alumina surrounded by MnS

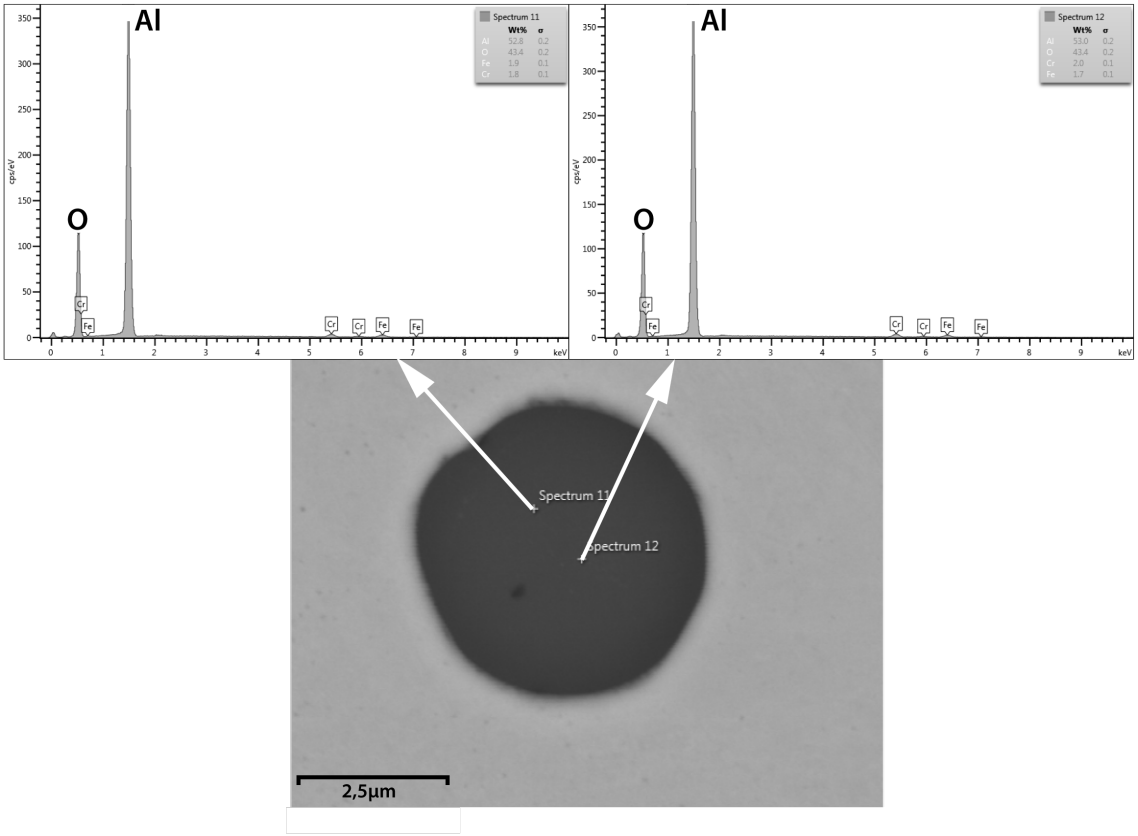

Figure 4.34: Defects in Batches 2 and 3. Spherical alumina inclusion

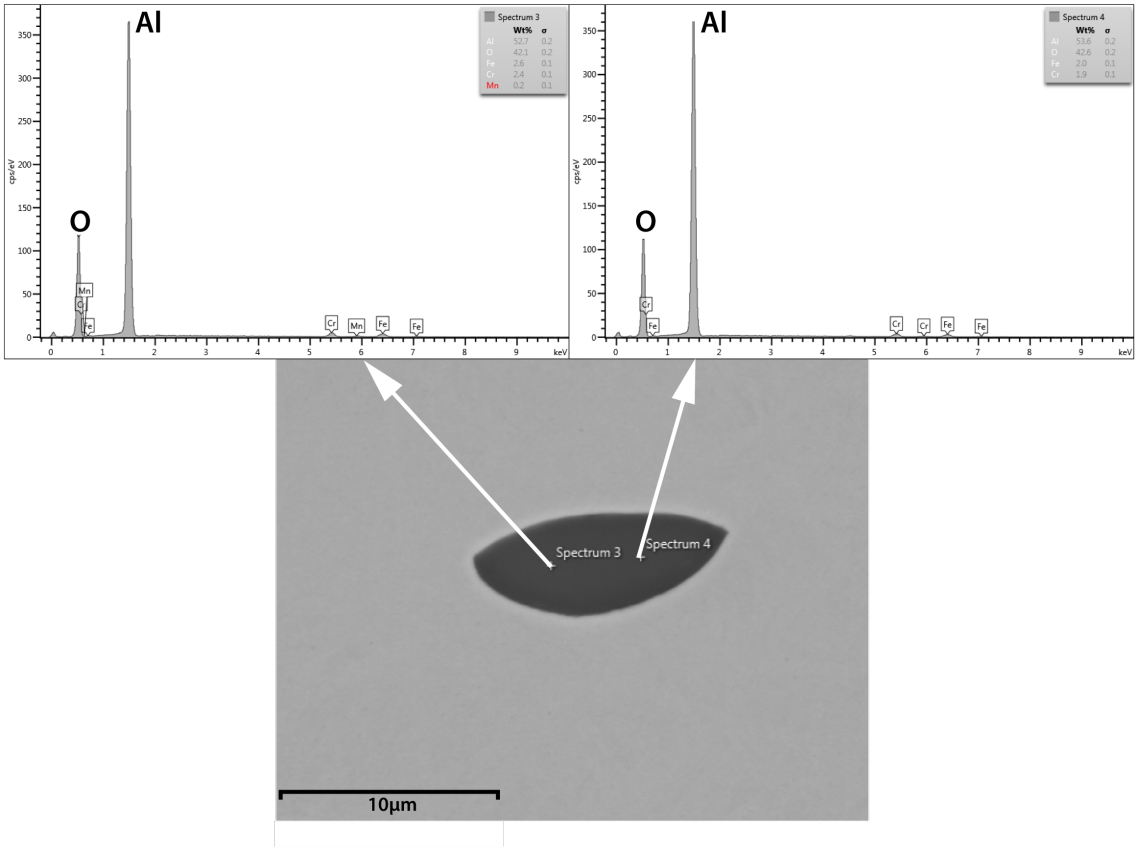

Figure 4.35: Defects in Batches 2 and 3. Elongated alumina inclusion

4.7 Defect Evaluation

Table 4.11: SS111116[10] defect equivalency defect size.

	Magnification	Defect size range (μm)	Defect morphology
DH 22.6	x100	22,6 - 45,3	spherical
DM 11.3	x100	11,3 - 22,5	spherical
DM 5.7	x200	5,7 - 11,2	spherical
DT 2.8	x200	2,9 - 5,6	spherical
AM 5.7	x200	5,7 - 11,2	stringer
AT 2.8	x200	5,7 - 11,2	stringer

Table 4.12: Defect sizes,morphology and densities in accordance with Swedish standard SS 111116 [10]

R7 BATCH 1	DH22.6 ($defects/mm^2$)	0,00189
	DM11.3 ($defects/mm^2$)	0,01135
	DM5.7 ($defects/mm^2$)	0,04975
	DT2.8 ($defects/mm^2$)	0,08455
	AT2.8 ($defects/mm^2$)	0,02984
	AM5.7 ($defects/mm^2$)	0
0802 BATCH 2	DH22.6 ($defects/mm^2$)	0,00198
	DM11.3 ($defects/mm^2$)	0,05746
	DM5.7 ($defects/mm^2$)	0,27355
	DT2.8 ($defects/mm^2$)	0,99969
0502 BATCH 2	DH22.6 ($defects/mm^2$)	0,00303
	DM11.3 ($defects/mm^2$)	0,05762
	DM5.7 ($defects/mm^2$)	0,27852
	DT2.8 ($defects/mm^2$)	1,28319
0601 BATCH 2	DH22.6 ($defects/mm^2$)	0,00164
	DM11.3 ($defects/mm^2$)	0,02462
	DM5.7 ($defects/mm^2$)	0,16413
	DT2.8 ($defects/mm^2$)	1,10911
0801 BATCH 3	DH22.6 ($defects/mm^2$)	0
	DM11.3 ($defects/mm^2$)	0,02578
	DM5.7 ($defects/mm^2$)	0,17408
	DT2.8 ($defects/mm^2$)	1,26329
0501 BATCH 3	DH22.6 ($defects/mm^2$)	0
	DM11.3 ($defects/mm^2$)	0,03372
	DM5.7 ($defects/mm^2$)	0,25365
	DT2.8 ($defects/mm^2$)	0,93006
0602 BATCH 3	DH22.6 ($defects/mm^2$)	0
	DM11.3 ($defects/mm^2$)	0,03775
	DM5.7 ($defects/mm^2$)	0,17408
	DT2.8 ($defects/mm^2$)	1,16879

4.8 Surface roughness

Table 4.13: Surface roughness

	$R_a(nm)$	$R_z(nm)$
Sample R6 *Batch*1	16,7	117,8
Sample 0101 *Batch*2	12,1	84,5
Sample 0301 *Batch*3	9,6	72,8

5

Discussion

5.1 Microstucture, hardness and strength differences between batches

The different manufacturing methods have produced different microstructure, mainly different retained austenite contents. This has influenced mechanical properties such as hardness, yield strength and UTS values for the different batches.
By looking at the hardness values from table 4.7 or retained austenite values from table 4.9, it can be said that the differences between batches existed before the final ageing HT, with samples 1001 and 0402 showing higher retained austenite and lower hardness than samples 1002 and 0401. Therefore batch 2 ultimately reached higher hardness than batch 3 after ageing. Strength differences seen in the tensile tests (figure 4.1) can be explained for the same reason, a lower retained austenite content in batch 2 than batch 3. This austenite is retained during the quenching of the solution HT and hipping for batches 2 and 3 respectively.
Finally it must be mentioned that the reference material showed the best performance in terms of strength and hardness due to the lowest retained austenite content. Despite batches 2 and 3 having smaller grain than batch 1, this one performed better. The fact that the tensile test was performed aligning the sample to the forging direction could benefit the strength measurements. However higher hardness values, where the forging direction does not come into play, still show a better performance for Batch 1, thus strengthening the fact that a better performance is linked to lower retained austenite contents.

5.2 Inclusions and defects differences between batches

The different manufacturing methods for the different batches produce different types of inclusions in the material. This inclusions have been documented in micrography, SEM images and their composition EDX analyzed. Their amount, size and morphology quantified (table 4.12)
From the results, differences between Batch 1 and batches 2 and 3 exist but not so much between batches 2 and 3. The main difference is that batch 1 show far less alumina inclusions than the AM batches. However Batch 1 show manganese sulfide (MnS) inclusions. These MnS inclusions manifest themselves in an elongated morphology due to the forging process. As mentioned previously fatigue and tensile tests

are carried out with samples aligned with their forging direction thus this elongated and unfavourable morphology may have not show any hindrance in performance but in a real life scenario where fatigue cycles can occur in any direction this may play a bigger role.
Defects found in Batches 2 and 3 are the same in both amount size and type. They are mainly spherical alumina 5-7μm and some bigger more oval-shaped alumina in the range of 10 μm size. No unmelted zones or voids were found. By the results, it can be said that hipping does not reduce the presence of alumina defects in the material as alumina has a high melting point. If voids or partially unmelted defects were present, perhaps hipping would reduce them but this is not the case for our batches since a fully dense material is obtained from the PBLS process.
Overall differences between batches when it comes to defects are little and so is their effect on fatigue performance.

5.3 Fatigue performance and its differences between batches

The manufacturing differences between batches show some differences in fatigue performance but these are little and some statistically not relevant.
Common behaviours for material can be found irrespective of their manufacturing process. By looking at results from Stress amplitude to number of cycles, the material shows a softening behaviour specially for 1.0% and 0.8% samples. This behaviour can also be observed by the reduction of stress that takes to complete a hysteresis loop as sample life advances.
The fact that ductility exponent c from the Coffin-Manson equations range around -0.55 denotes a long fatigue life expectancy for this material. The ductility exponent c normally ranges between -0.5 and -0.7. Previous studies on similar maraging steels agree with this result.
Difference between the batches exist although the amount of samples tested are not enough to confirm these differences and make them statistically meaningful. The main difference are that Batches 1 and 2 show higher stress levels for the same strain as their yield strength and UTS values are higher. Batch 3 show less scatter. Fatigue life seem to be better for batch 1 then 2 and finally 3. This is compatible to what has been previously discussed in regards to retained austenite, hardness and strength values.
Strain levels of 0.8% and 0.6% are too elastic for batches 1 and 2 and thus the scattering is higher than that for batch 3 where the material has a higher plastic component of strain at those strain amplitude levels. More samples at higher strain amplitude levels should have been tested but buckling/load cell limitations existed in the tests. The fact is 0.6 % strain amplitude tests are almost fully elastic and thus number of cycles to failure occur with high scatter. This is the reason why C-M equations were built excluding these samples as they belong more to the HCF and Basquin equation zone of the curve.
In figure 4.9 the C-M equations for the three batches are shown along with the 95% prediction interval for batch 1. From this figure the following can be stated: All

batches show very similar Fatigue life expectancy and that no statistical meaningful difference exist between them. The AM manufactured samples from both batches 2 and 3 can reach equally high fatigue performance as the forged samples that constitute batch 1 if the heat treatments are correct. More tests are needed to confirm that strengthen the fact that the performance is equally as good or reduce the confidence intervals of the batches until they do not overlap proving that they are different, this would take many samples as the averages run almost on top of each other.

5.4 Fracture mechanisms

Fractography results show that fracture mechanisms are very similar between batches, being identical for batches 2 and 3.
Stereomicroscope images from the fracture zones show that as expected, samples tested at higher strain amplitude show smaller crack growth area. This is because a larger area reduction due to a crack can be stable if stresses are smaller.
Batches 2 and 3 present flatter fracture surfaces and cleaner while batch 1 shows more faceted fracture surfaces where the crack advanced in different directions. For all batches fractures can be described as ductile fractures with a big fibrous rupture zone and clear shear lips.
SEM analysis attempted to conclude the cause for crack initiation point (CIP) and link the it to those defects studied previously. Although some CIP were identified and examined in samples from all batches, no clear conclusion could be drawn as to if a defect caused it.

6
Conclusions

Different manufacturing methods produce differences in microstructure and mechanical properties.
Hardness, strength, retained austenite readings and stress amplitude to number of cycles results strengthen the fact that these different manufacturing methods affect properties.
The different manufacturing methods are well represented by batches 1, 2 and 3. However more samples and at higher strain amplitude levels would have been desirable.
Fatigue data analysis show that Corrax® and Corrax AM® show great fatigue performance and that no differences seem to exist as the differences found are not statistically significant.
Hipping gives no additional advantage over a normal solution HT in terms of mechanical properties or fatigue performance. Furthermore the different quenching process in HIP may have caused an increase of retained austenite as compared to batch 2 which has shown detrimental in terms of mechanical properties.
The Additive manufacturing processing of Corrax AM® (Batches 2 and 3) show a very clean and consistent material comparable to that of Corrax® (Batch 1). This is linked to the statistically identical fatigue life expectancy of all three batches.

7
Future Research

After the discussion and conclusions previously exposed, some of the initial questions which this thesis aimed to answer have been explained but others still remain. The behaviour of Corrax AM® to Hipping is known but possibilities such as processing Corrax AM® with coarser and cheaper parameters during the PBLM process to then recover the properties of a fully dense material during HIP has yet to be investigated in terms of fatigue performance. The commercial interest of this application is promising thus worth investigating.
Another line of research and natural continuation of this project would be the determination of the high cycle fatigue properties for Corrax AM®.

Bibliography

[1] www.Uddeholm.com/en/
20/08/2019

[2] ASTM E606/E606M-12 Standard Test Method for Strain-Controlled Fatigue testing.
04/03/2019

[3] Gibson, Ian, et al. Additive Manufacturing Technologies. 2nd ed., Springer.

[4] Christos Oikonomou, Seshendra Karamchedu ,Uddeholms AB, SE 683 85 Hagfors, Sweden

[5] Popov, Vladimir Katz-Demyanetz, Alexander Garkun, Andrey Muller-Kamskii, Gary Strokin, Evgeny Rosenson, H. (2018). Effect of Hot Isostatic Pressure treatment on the Electron-Beam Melted Ti-6Al-4V specimens. Procedia Manufacturing. 21. 125-132. 10.1016/j.promfg.2018.02.102.

[6] https://www.uddeholm.com/files/PB_Uddeholm_corrax_english.pdf
25/08/2019

[7] https://www.uddeholm.com/app/uploads/sites/36/2017/08/AM-Corrax-english_1705_e1.pdf
25/08/2019

[8] Additive manufacturing-System performance and reliability-Standard test method for acceptance of powder-bed fusion machines for metallic materials for aerospace application, ISO/ASTM DIS 52941:2019(E).

[9] Influence of non-metallic inclusions on the fatigue properties of heavily cold drawn steel wires. Kasper Lambrighs, Ignaas Verpoest, Bert Verlinden, Martine Wevers. Elsevier 2010

[10] Jernkontoret's inclusion chart II for quantitative assessment of the content of non-metallic inclusions in metals and alloys
https://www.sis.se/api/document/preview/80009489/
25/08/2019

[11] https://www.sciencedirect.com/topics/chemistry/maraging-steel
22/08/2019

[12] ASM International, Metals Handbook, Mechanical Testing, 1985, Ninth Edition, Volume 8

[13] ASTM E407 - 07(2015)e1 ,Standard Practice for Microetching Metals and Alloys.

A

Appendix 1. Hysteresis loops for all samples

A.1 Batch 1

A.1.1 Sample R2 1.0% strain Amplitude. 137 cycles to failure

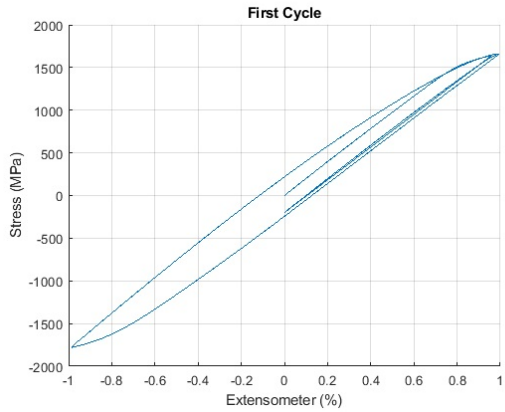

Figure A.1: Sample R2. First cycle

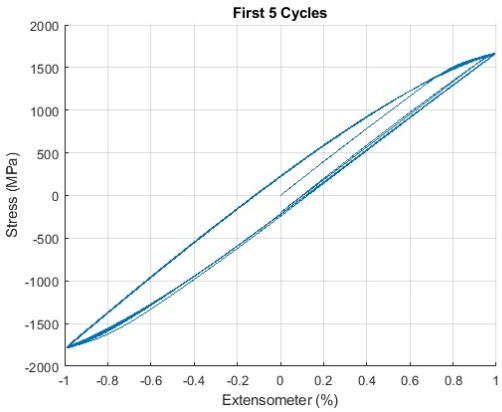

Figure A.2: Sample R2. First 5 cycles

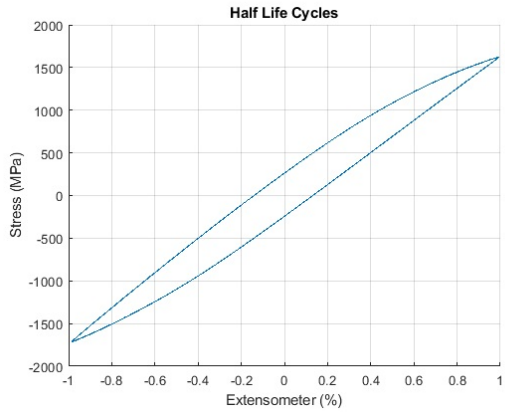

Figure A.3: Sample R2. Half life cylces

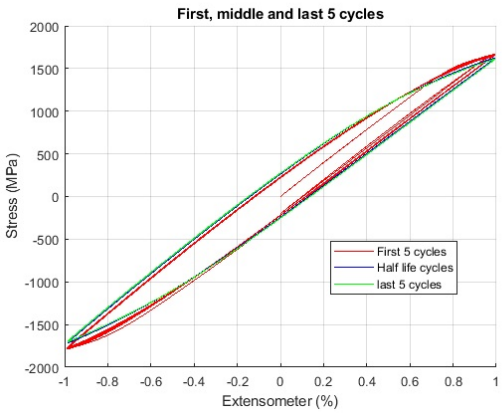

Figure A.4: Sample R2. 5 first, 5 half life and 5 last cycles

A.1.2 Sample R8 1.0% strain Amplitude. 483 cycles to failure

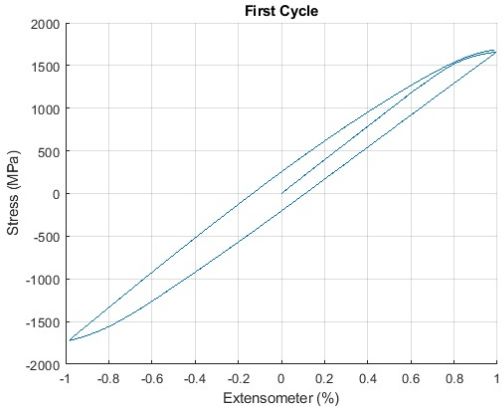

Figure A.5: Sample R8. First cycle

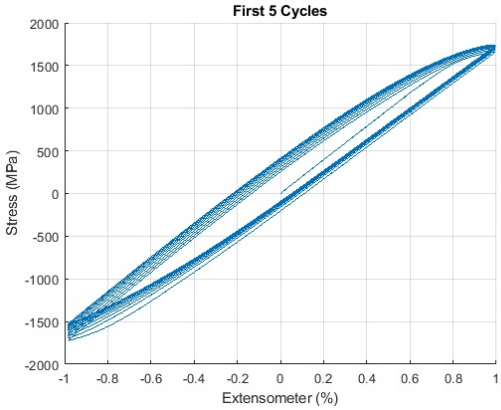

Figure A.6: Sample R8. First 5 cycles

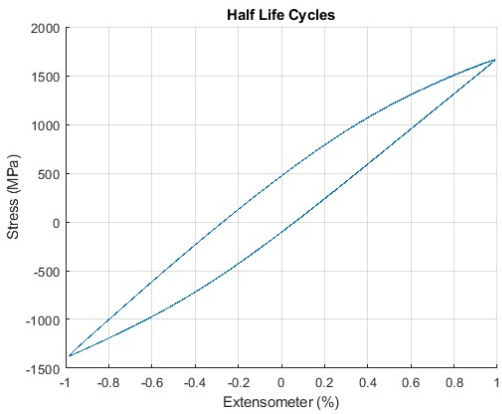

Figure A.7: Sample R8. Half life cylces

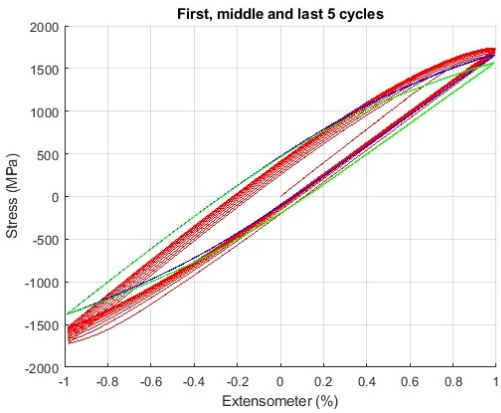

Figure A.8: Sample R8. 5 first, 5 half life and 5 last cycles

A.1.3 Sample R9 1.0% strain Amplitude. 401 cycles to failure

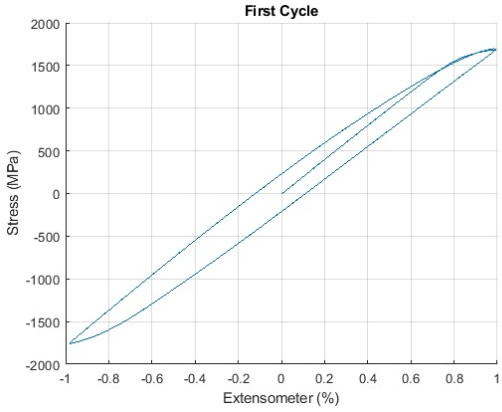

Figure A.9: Sample R9. First cycle

1/R9/First 5 cycles R9.jpg

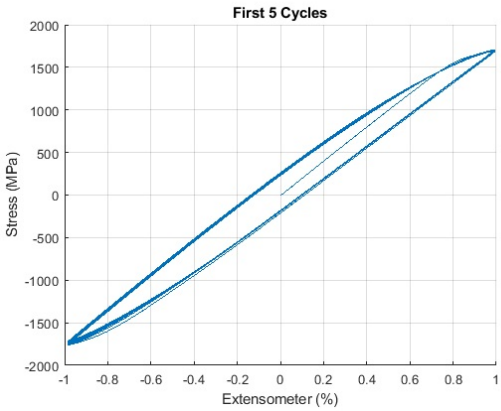

Figure A.10: Sample R9. First 5 cycles

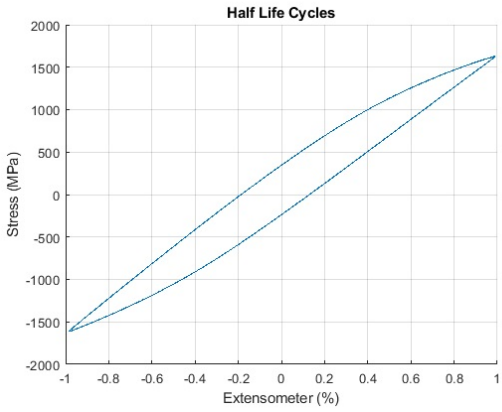

Figure A.11: Sample R9. Half life cycles

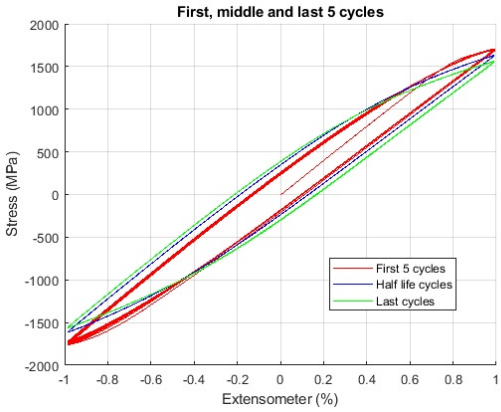

Figure A.12: Sample R9. 5 first, 5 half life and 5 last cycles

A.1.4 Sample R4 0.8% strain Amplitude. 1887 cycles to failure

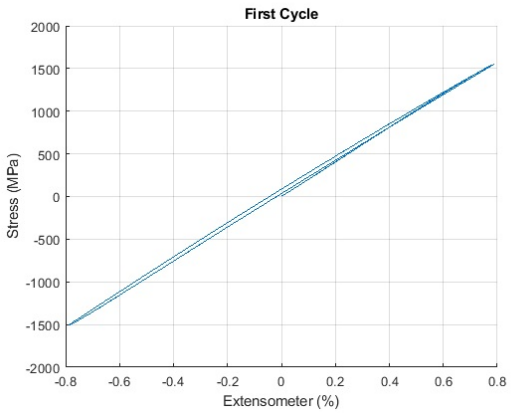

Figure A.13: Sample R4. First cycle

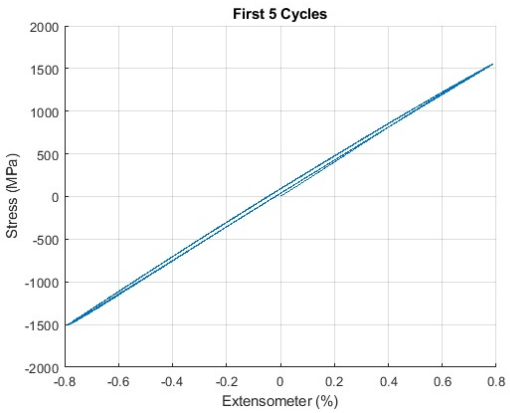

Figure A.14: Sample R4. First 5 cycles

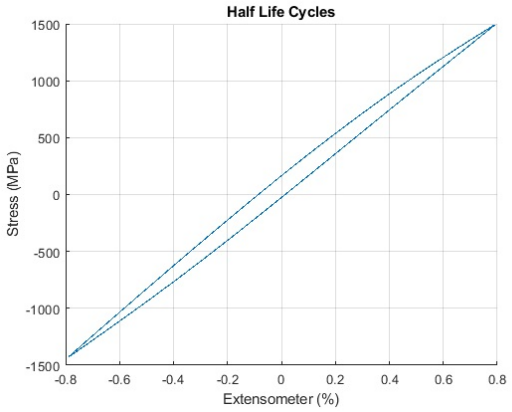

Figure A.15: Sample R4. Half life cycles

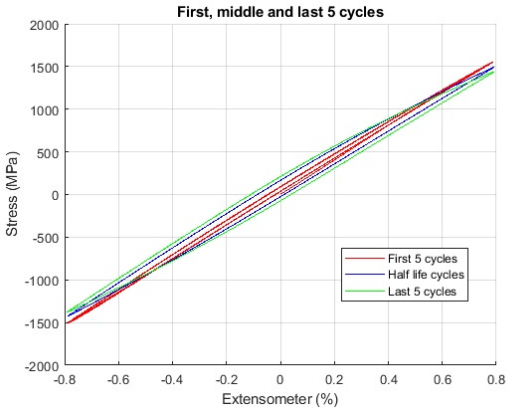

Figure A.16: Sample R4. 5 first, 5 half life and 5 last cycles

A.1.5 Sample R6 0.8% strain Amplitude. 724 cycles to failure

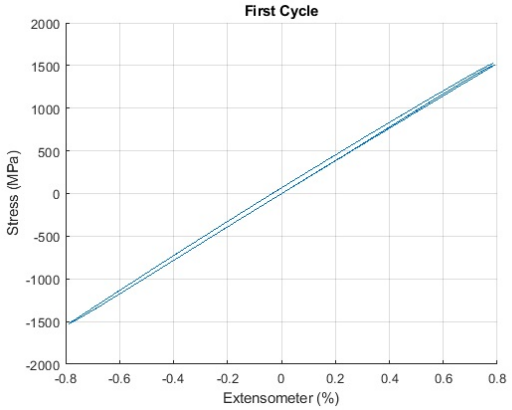

Figure A.17: Sample R6. First cycle

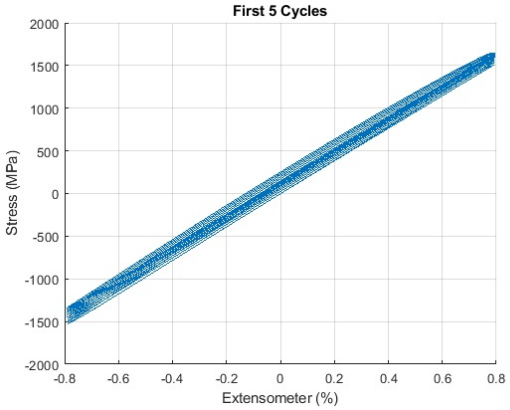

Figure A.18: Sample R6. First 5 cycles

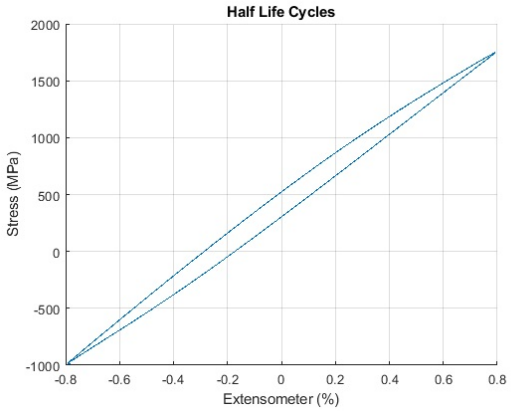

Figure A.19: Sample R6. Half life cycles

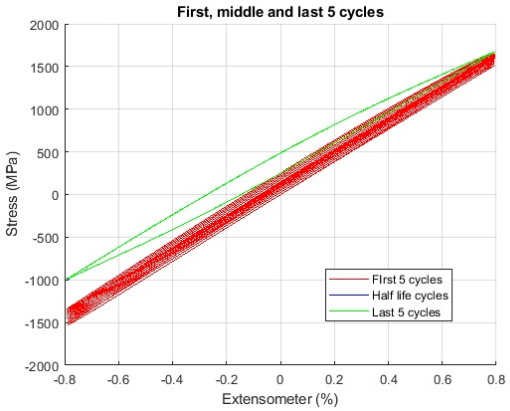

Figure A.20: Sample R6. 5 first, 5 half life and 5 last cycles

A.1.6 Sample R3 0.6% strain Amplitude. 13870 cycles to failure

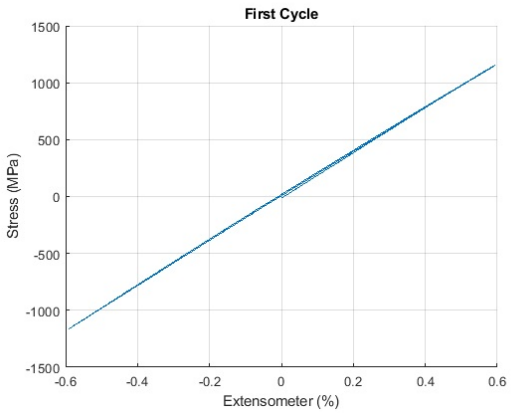

Figure A.21: Sample R3. First cycle

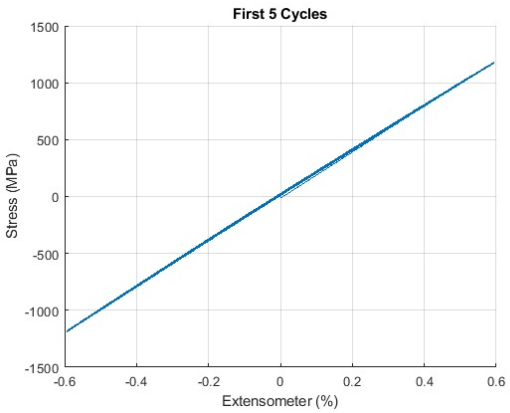

Figure A.22: Sample R3. First 5 cycles

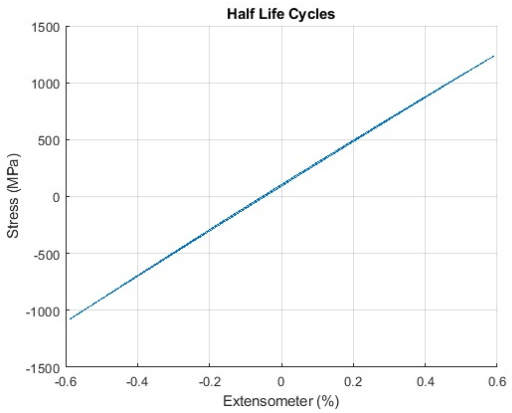

Figure A.23: Sample R3. Half life cycles

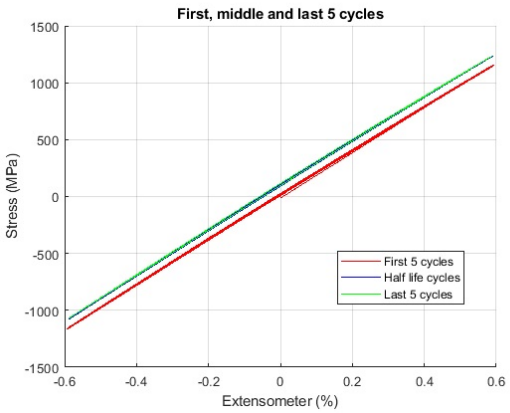

Figure A.24: Sample R3. 5 first, 5 half life and 5 last cycles

A.1.7 Sample R5 0.6% strain Amplitude. 7411 cycles to failure

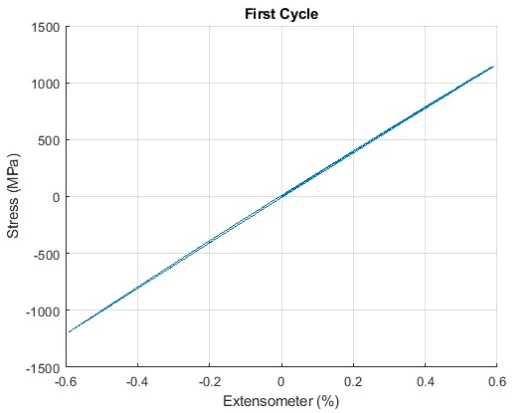

Figure A.25: Sample R5. First cycle

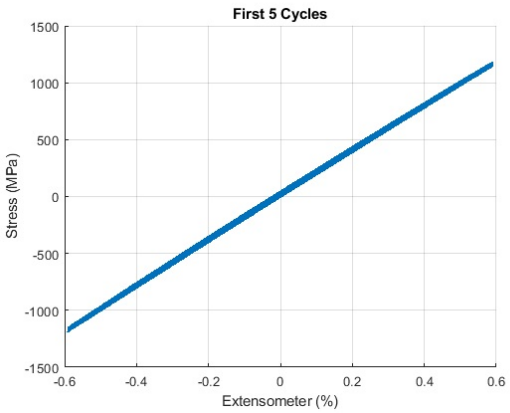

Figure A.26: Sample R5. First 5 cycles

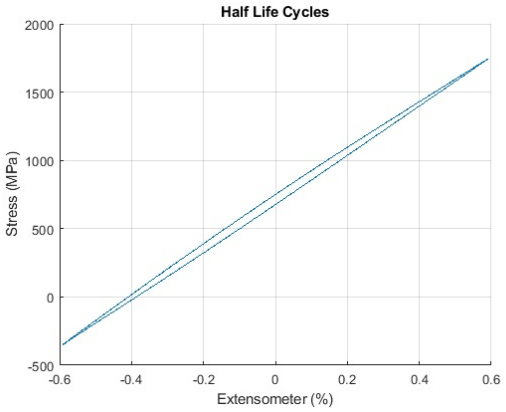

Figure A.27: Sample R5. Half life cycles

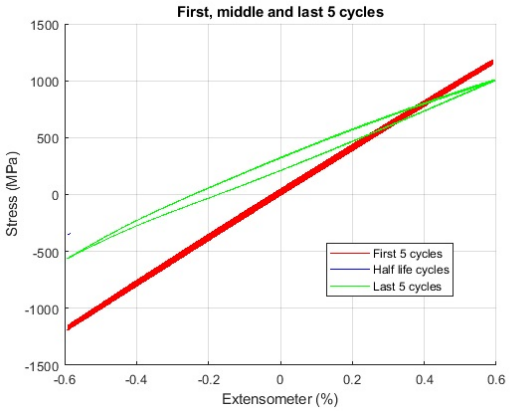

Figure A.28: Sample R5. 5 first, 5 half life and 5 last cycles

A.2 Batch 2

A.2.1 Sample 0302 1.0% strain Amplitude. 252 cycles to failure

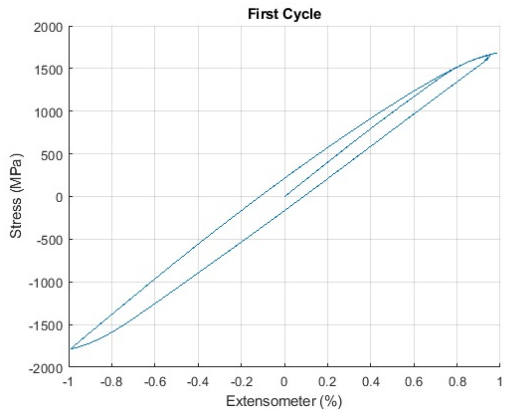

Figure A.29: Sample 0302. First cycle

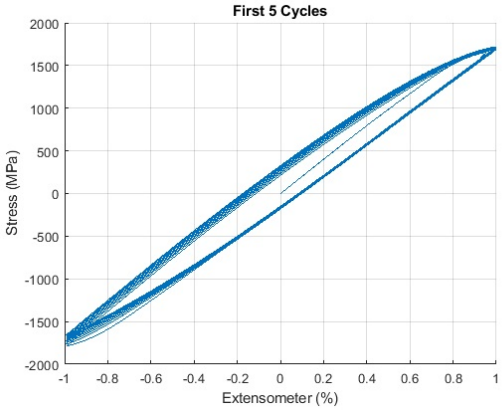

Figure A.30: Sample 0302. First 5 cycles

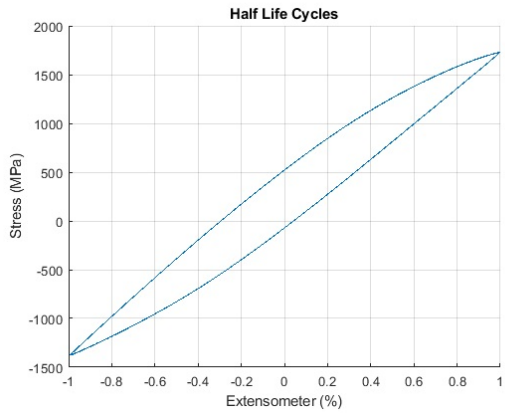

Figure A.31: Sample 0302. Half life cycles

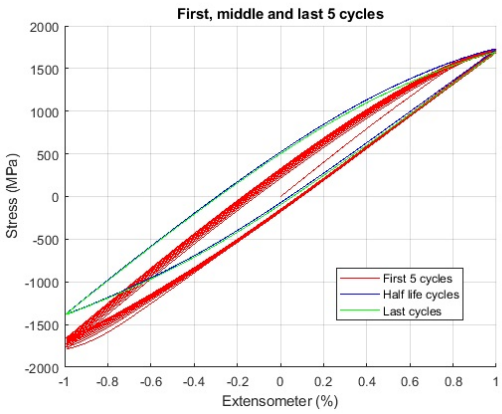

Figure A.32: Sample 0302. 5 first, 5 half life and 5 last cycles

A.2.2 Sample 0601 1.0% strain Amplitude. 180 cycles to failure

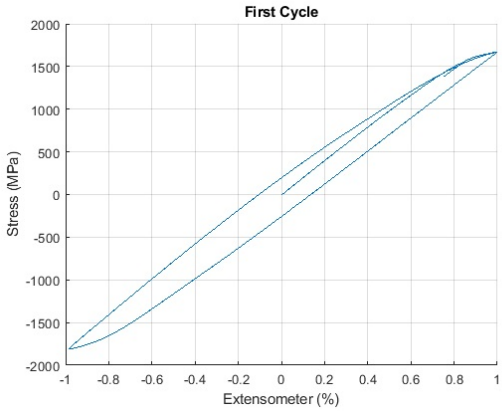

Figure A.33: Sample 0601. First cycle

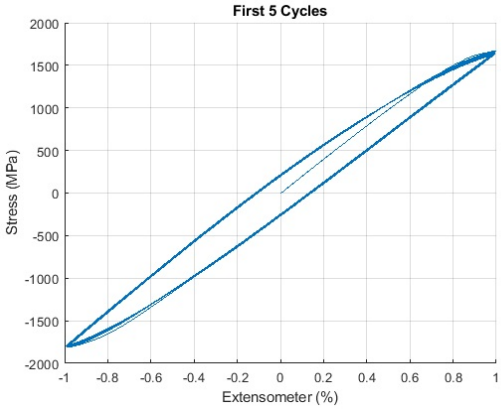

Figure A.34: Sample 0601. First 5 cycles

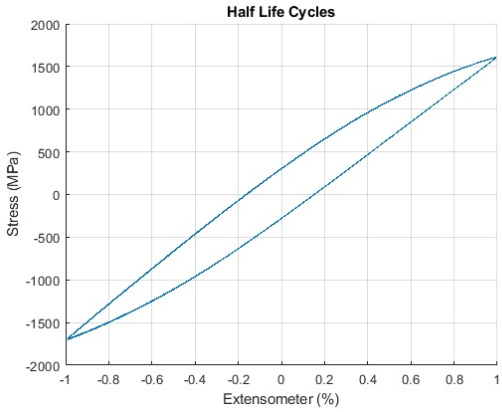

Figure A.35: Sample 0601. Half life cycles

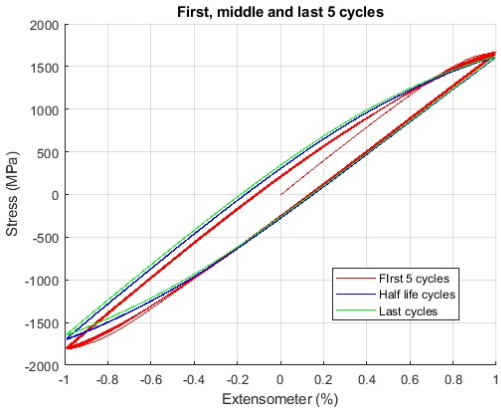

Figure A.36: Sample 0601. 5 first, 5 half life and 5 last cycles

A.2.3 Sample 1002 0.8% strain Amplitude. 547 cycles to failure

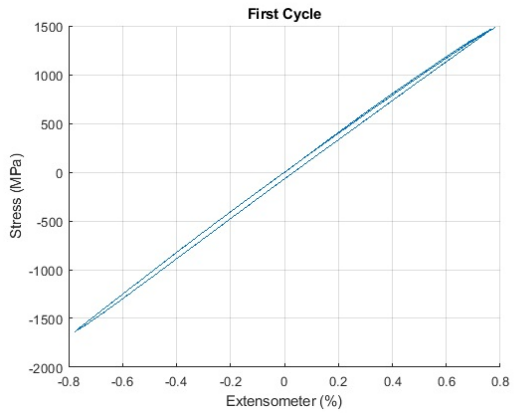

Figure A.37: Sample 1002. First cycle

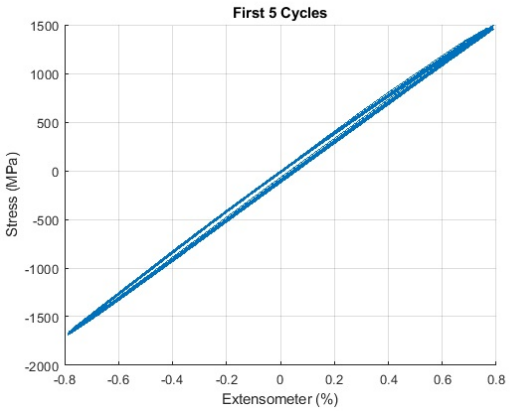

Figure A.38: Sample 1002. First 5 cycles

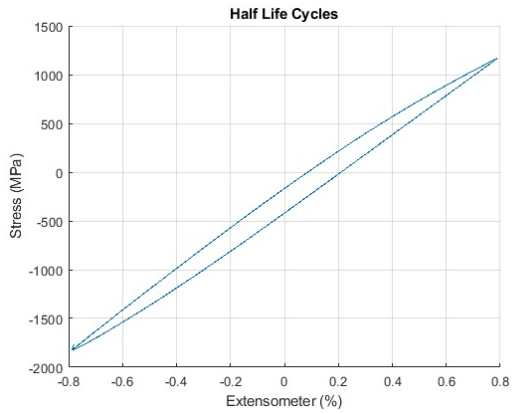

Figure A.39: Sample 1002. Half life cycles

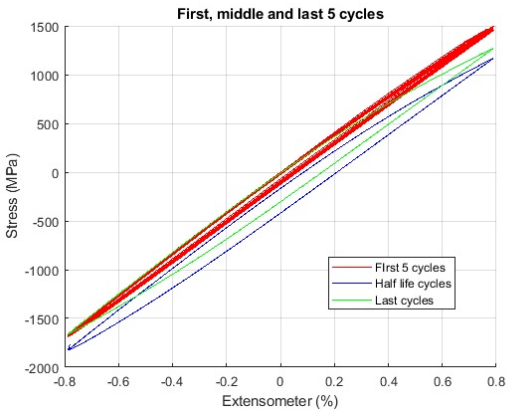

Figure A.40: Sample 1002. 5 first, 5 half life and 5 last cycles

A.2.4 Sample 0101 0.8% strain Amplitude. 1187 cycles to failure

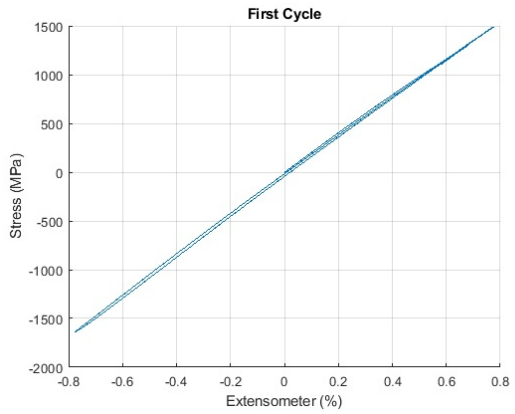

Figure A.41: Sample 0101. First cycle

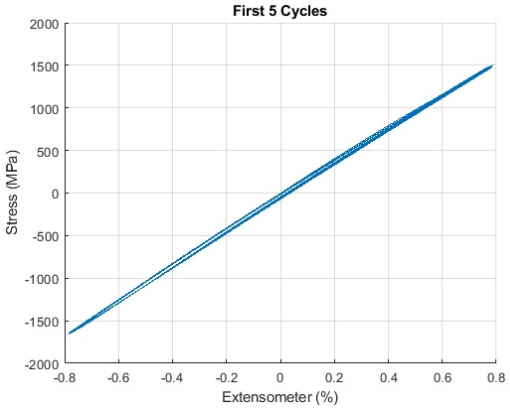

Figure A.42: Sample 0101. First 5 cycles

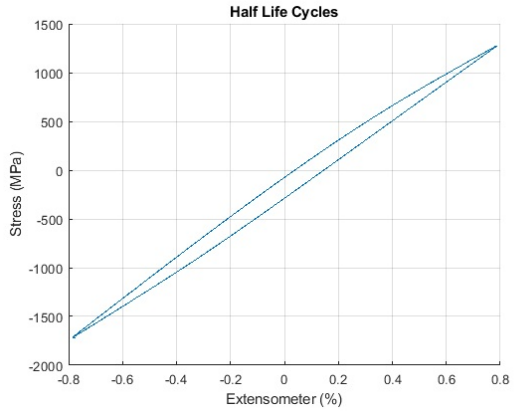

Figure A.43: Sample 0101. Half life cycles

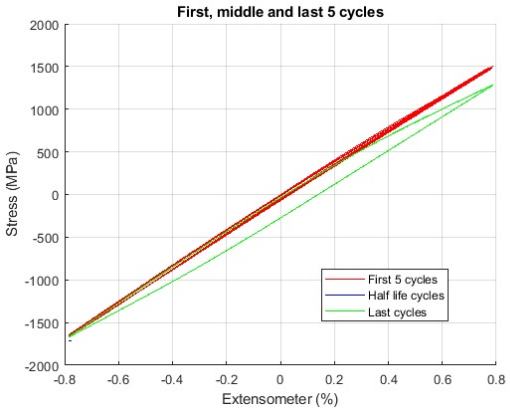

Figure A.44: Sample 0101. 5 first, 5 half life and 5 last cycles

A.2.5 Sample 0701 0.8% strain Amplitude. 1850 cycles to failure

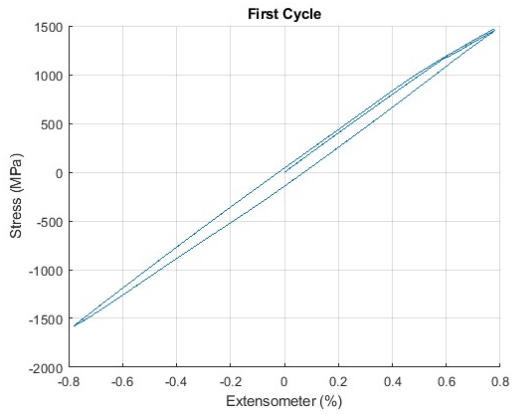

Figure A.45: Sample 0701. First cycle

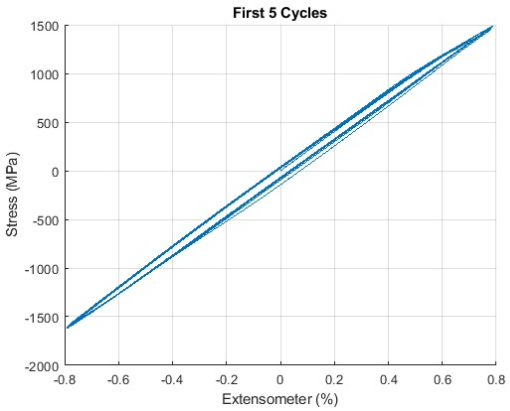

Figure A.46: Sample 0701. First 5 cycles

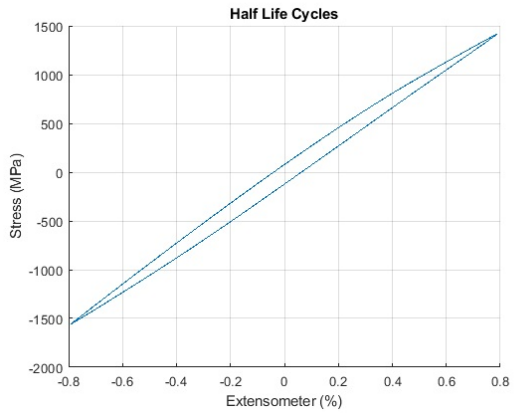

Figure A.47: Sample 0701. Half life cycles

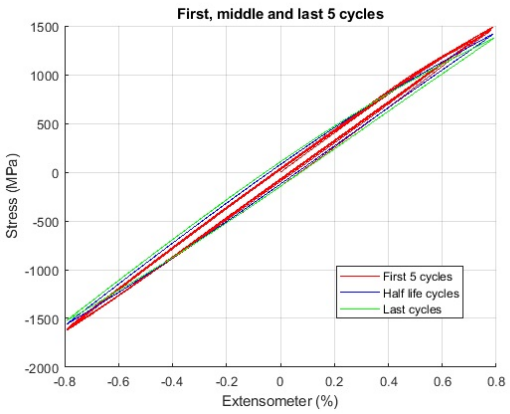

Figure A.48: Sample 0701. 5 first, 5 half life and 5 last cycles

A.2.6 Sample 0502 0.6% strain Amplitude. 20010 cycles to failure

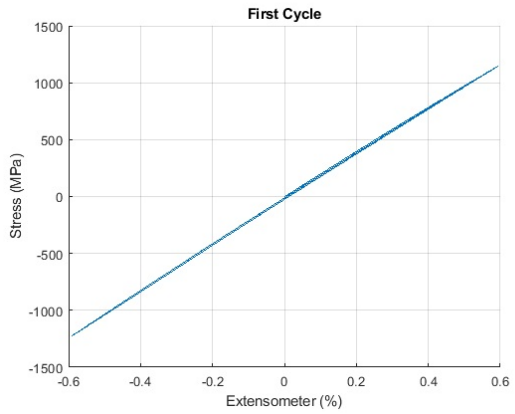

Figure A.49: Sample 0502. First cycle

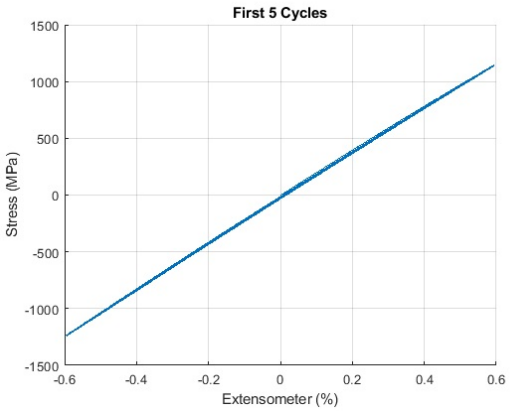

Figure A.50: Sample 0502. First 5 cycles

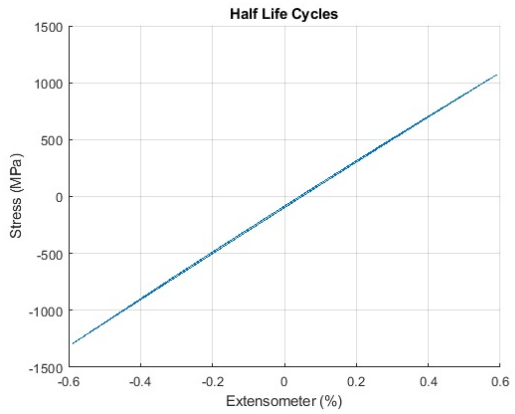

Figure A.51: Sample 0502. Half life cycles

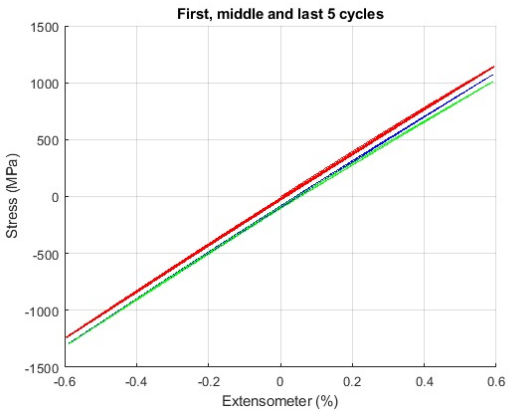

Figure A.52: Sample 0502. 5 first, 5 half life and 5 last cycles

A.2.7 Sample 0901 0.6% strain Amplitude. 13852 cycles to failure

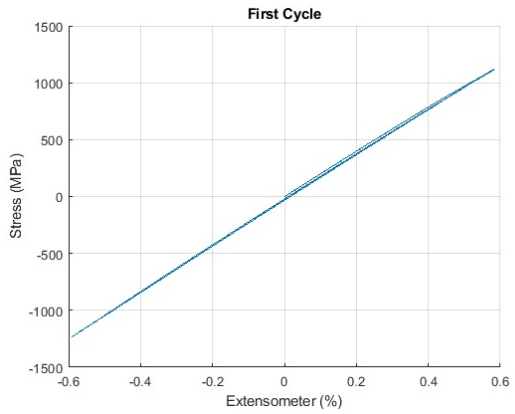

Figure A.53: Sample 0901. First cycle

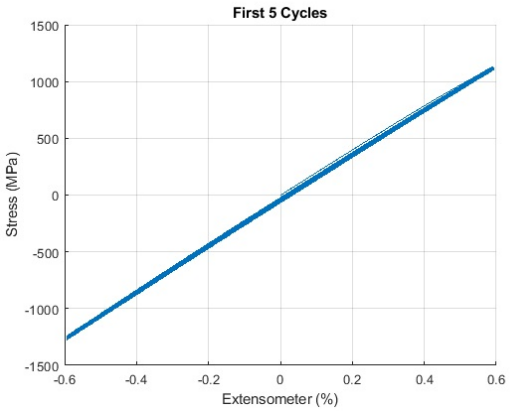

Figure A.54: Sample 0901. First 5 cycles

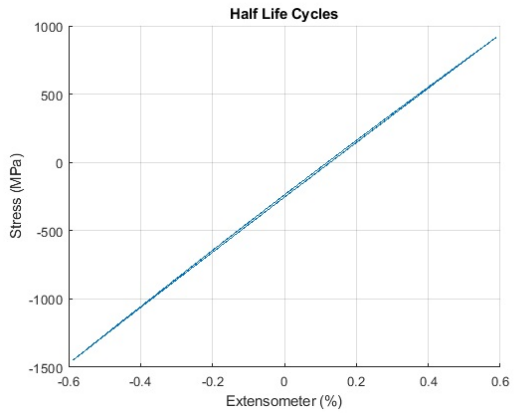

Figure A.55: Sample 0901. Half life cycles

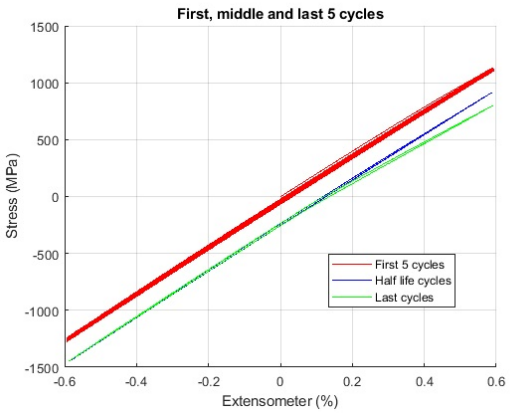

Figure A.56: Sample 0901. 5 first, 5 half life and 5 last cycles

A.3 Batch 3

A.3.1 Sample 0301 1.0% strain Amplitude. 173 cycles to failure

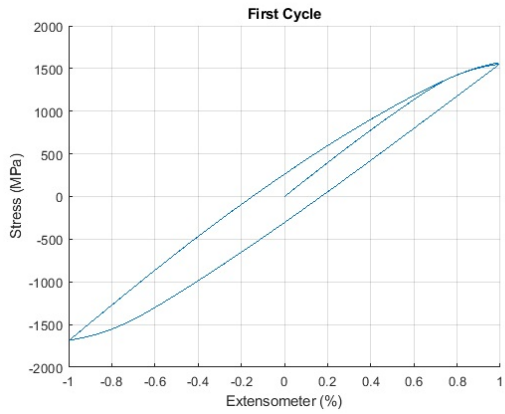

Figure A.57: Sample 0301. First cycle

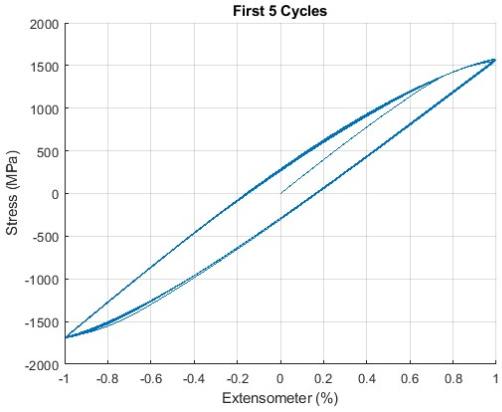

Figure A.58: Sample 0301. First 5 cycles

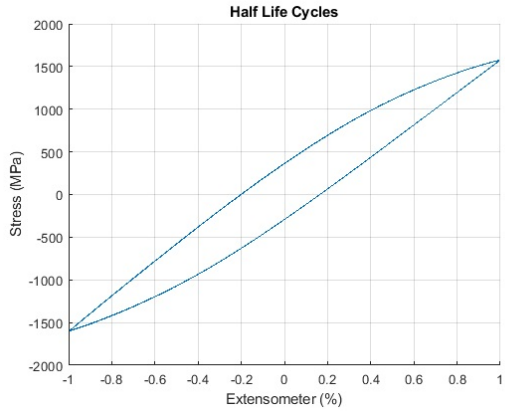

Figure A.59: Sample 0301. Half life cycles

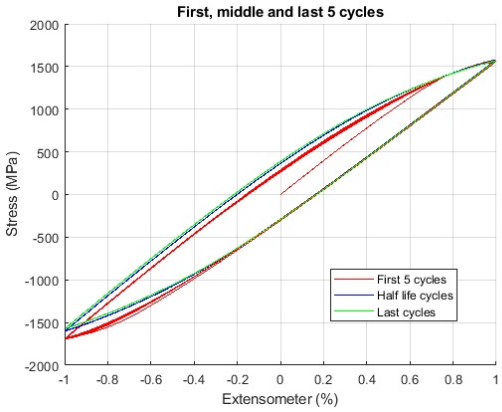

Figure A.60: Sample 0301. 5 first, 5 half life and 5 last cycles

A.3.2 Sample 0602 1.0% strain Amplitude. 126 cycles to failure

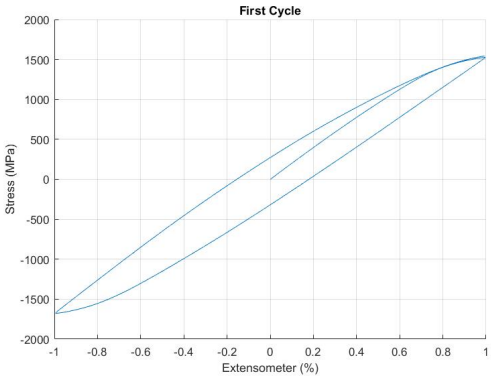

Figure A.61: Sample 0602. First cycle

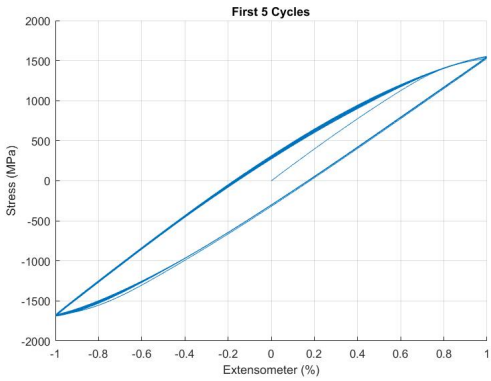

Figure A.62: Sample 0602. First 5 cycles

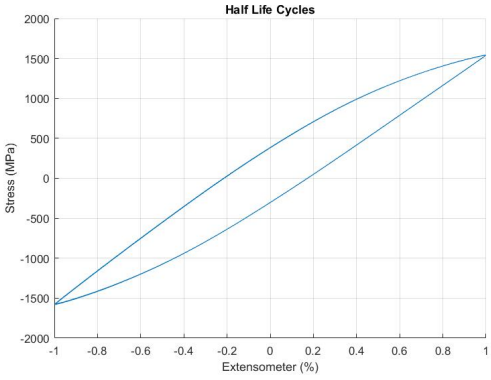

Figure A.63: Sample 0602. Half life cycles

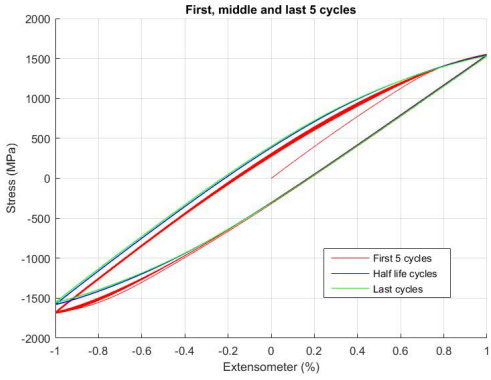

Figure A.64: Sample 0602. 5 first, 5 half life and 5 last cycles

A.3.3 Sample 0801 1.0% strain Amplitude. 300 cycles to failure

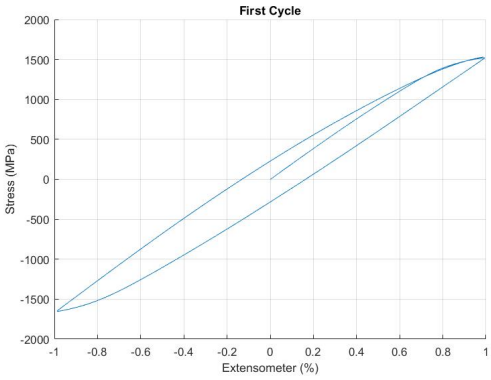

Figure A.65: Sample 0801. First cycle

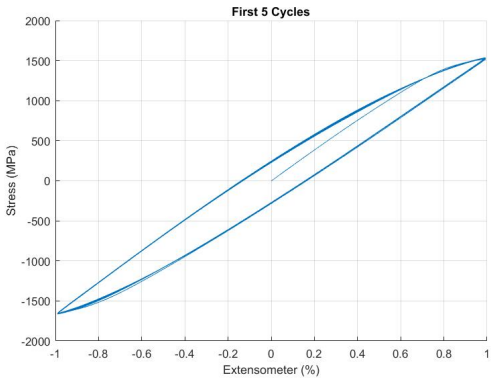

Figure A.66: Sample 0801. First 5 cycles

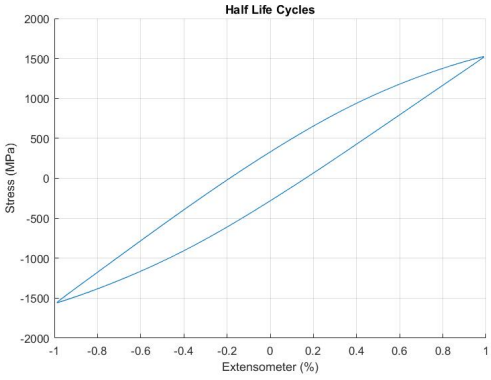

Figure A.67: Sample 0801. Half life cycles

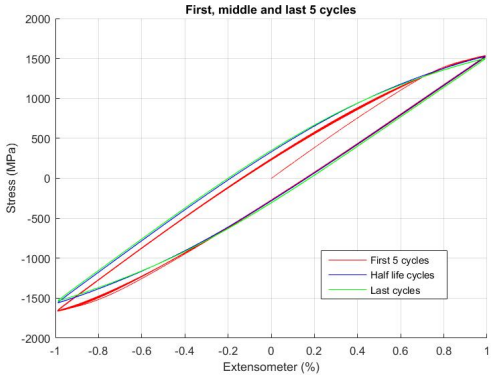

Figure A.68: Sample 0801. 5 first, 5 half life and 5 last cycles

A.3.4 Sample 0102 0.8% strain Amplitude. 600 cycles to failure

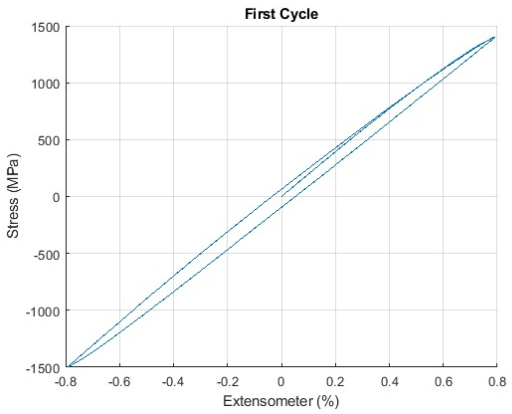

Figure A.69: Sample 0102. First cycle

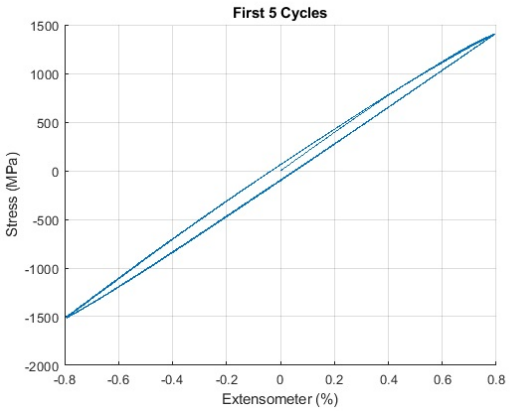

Figure A.70: Sample 0102. First 5 cycles

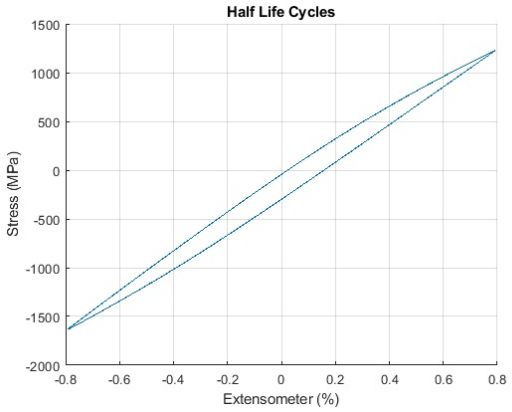

Figure A.71: Sample 0102. Half life cycles

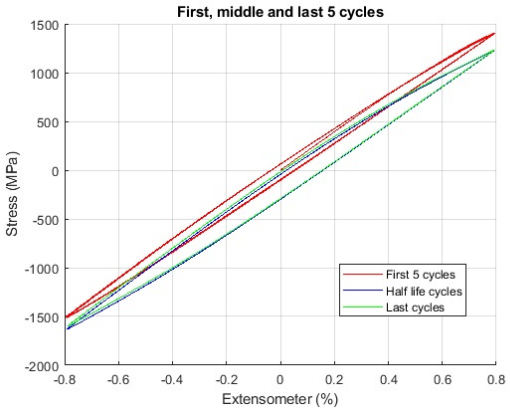

Figure A.72: Sample 0102. 5 first, 5 half life and 5 last cycles

A.3.5 Sample 1001 0.8% strain Amplitude. 1283 cycles to failure

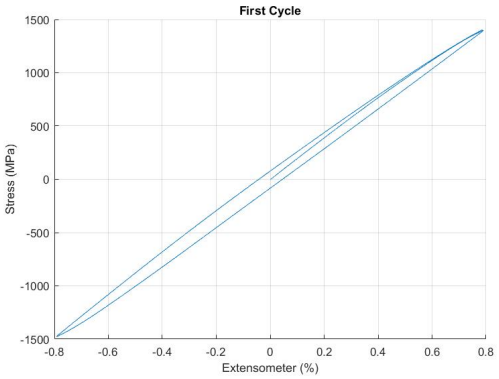

Figure A.73: Sample 1001. First cycle

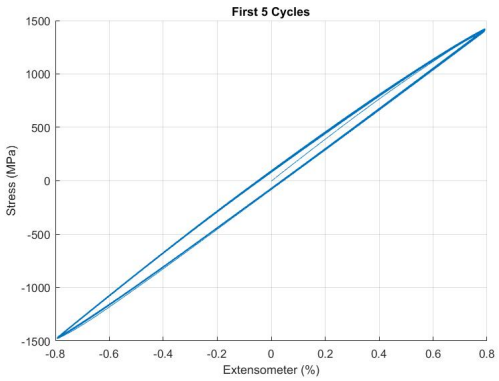

Figure A.74: Sample 1001. First 5 cycles

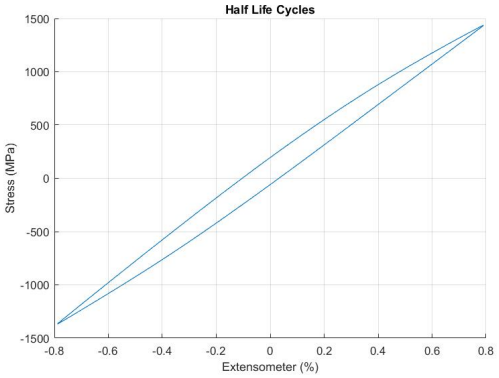

Figure A.75: Sample 1001. Half life cycles

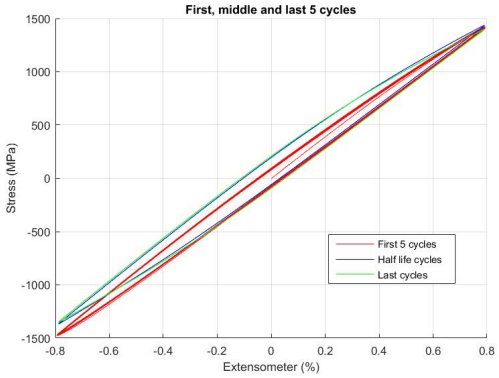

Figure A.76: Sample 1001. 5 first, 5 half life and 5 last cycles

A.3.6 Sample 0201 0.8% strain Amplitude. 884 cycles to failure

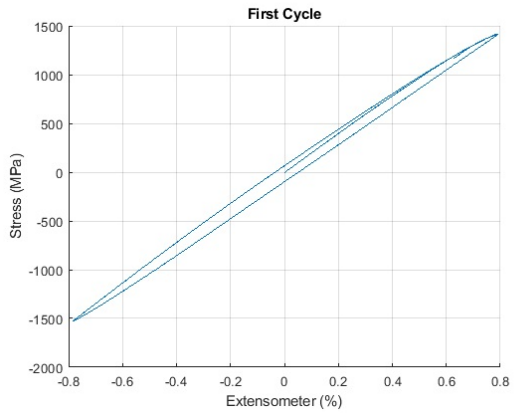

Figure A.77: Sample 0201. First cycle

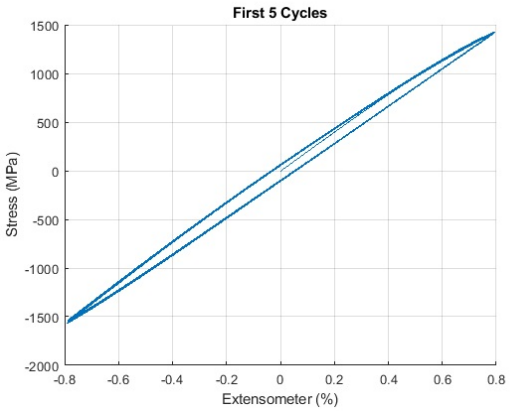

Figure A.78: Sample 0201. First 5 cycles

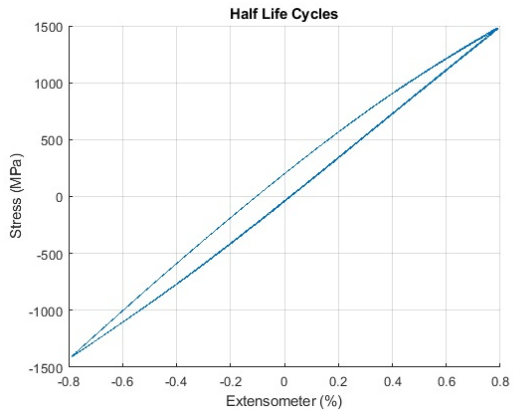

Figure A.79: Sample 0201. Half life cycles

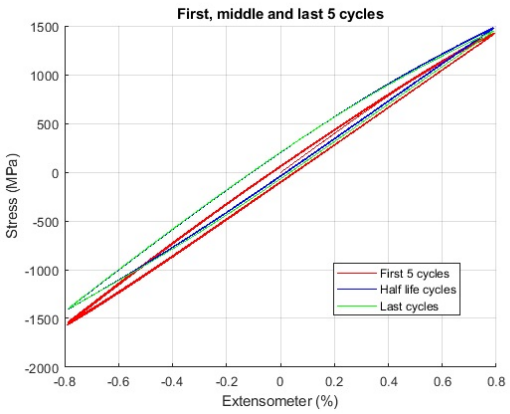

Figure A.80: Sample 0201. 5 first, 5 half life and 5 last cycles

A.3.7 Sample 0902 0.6% strain Amplitude. 9144 cycles to failure

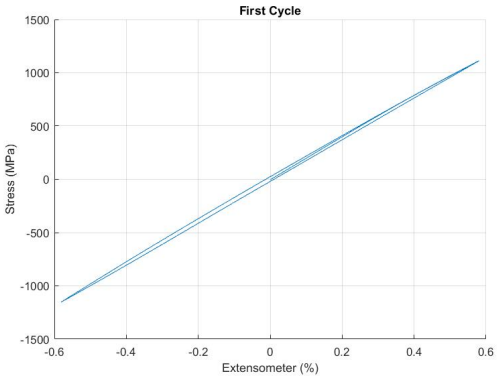

Figure A.81: Sample 0902. First cycle

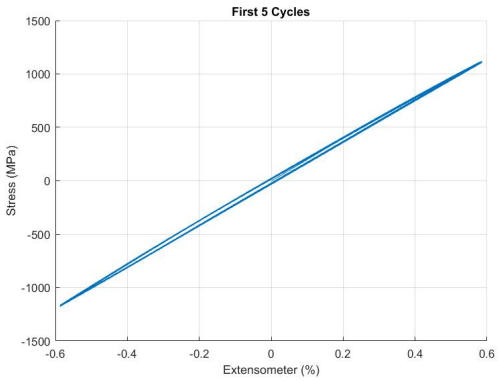

Figure A.82: Sample 0902. First 5 cycles

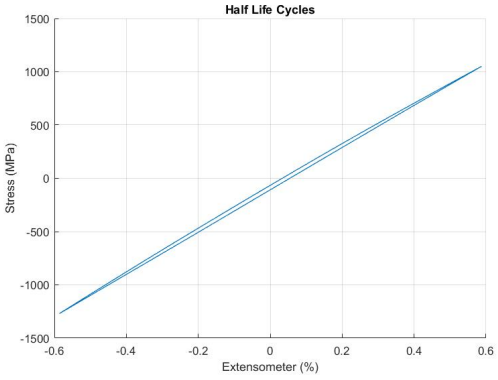

Figure A.83: Sample 0902. Half life cycles

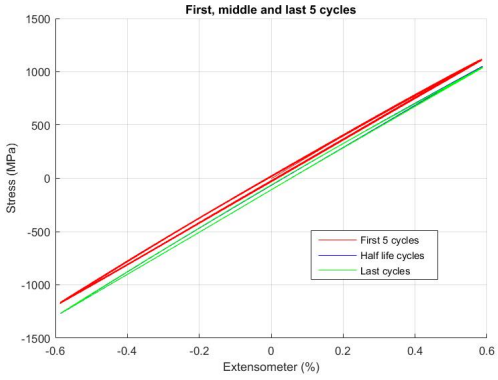

Figure A.84: Sample 0902. 5 first, 5 half life and 5 last cycles

A.3.8 Sample 0402 0.6% strain Amplitude. 5611 cycles to failure

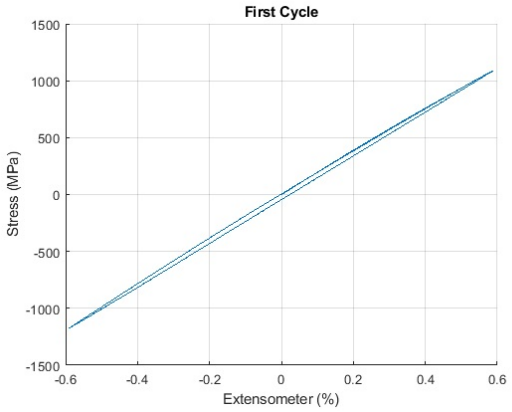

Figure A.85: Sample 0402. First cycle

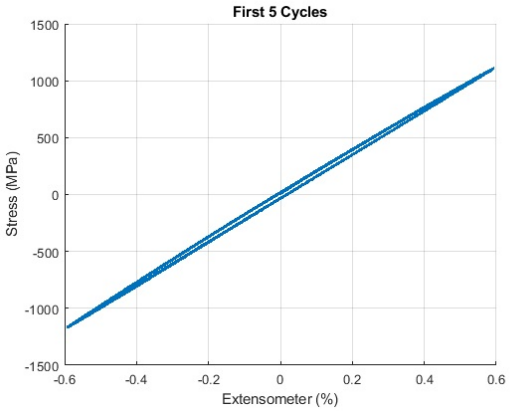

Figure A.86: Sample 0402. First 5 cycles

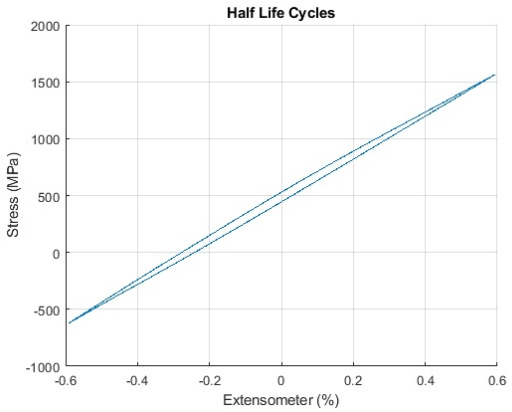

Figure A.87: Sample 0402. Half life cycles

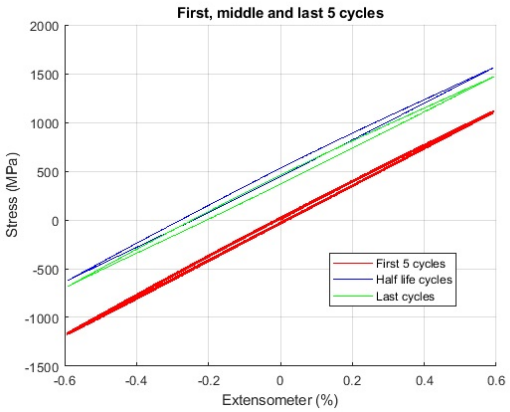

Figure A.88: Sample 0402. 5 first, 5 half life and 5 last cycles